Journal of Hydrology: Regional Studies 28 (2020) 100667

Contents lists available at ScienceDirect

Journal of Hydrology: Regional Studies

journal homepage: www.elsevier.com/locate/ejrh

Recharge pathways and rates for a sand aquifer beneath a loess-mantled landscape in western Tennessee, U.S.A.

Daniel Larsen[a,*], John Bursi[b], Brian Waldron[c], Scott Schoefernacker[c], James Eason[b]

[a] Department of Earth Science, University of Memphis, Memphis, TN 38152
[b] Department of Earth Sciences, University of Memphis, Memphis, TN 38152
[c] Center for Applied Earth Science and Engineering Research, University of Memphis, Memphis, TN 38152

ARTICLE INFO

Keywords:
Groundwater
Loess
Aquifer
Vertical infiltration
Lateral recharge

ABSTRACT

Study region: : Western Tennessee, U.S.A.
Study focus: : Recharge to aquifers that underlie loess and other fine-grained surficial deposits in western Tennessee as well as other areas is commonly impeded resulting in sensitivity in regard to sustainability of groundwater resources. This study investigates the role of preferential pathways of recharge to the regional Memphis aquifer in an area mantled by loess and fine-grained paleosols.
New hydrological insights: : Data gathered through a vadose-zone chloride mass balance analysis and a year of monitoring physical hydrologic, water chemistry, and environmental and applied tracer data within an upland watershed in western Tennessee indicate that recharge to the Memphis aquifer is dominated by lateral recharge of infiltrated stream water sources rather than vertical infiltration through loess-covered uplands. The results from this research challenge prevailing models of recharge to the Memphis aquifer and aquifers mantled by loess or other fine-grained soils in other regions that envision vertical recharge through fine-grained soils to be the dominant recharge mechanism.

1. Introduction

Surficial deposits of loess and reworked fine-grained sediment have potential to inhibit recharge to underlying aquifer systems, limiting sustainability of regional groundwater resources (Prill, 1977; Huang et al., 2017; Gerginov et al., 2018). Slow infiltration rates through loess and other fine-grained soils hinder downward movement of water through unsaturated zone profiles (Weinthal et al., 2005; Deng et al., 2015; Kalhoro et al., 2018), in part due to differences in vegetative cover (Dafny and Šimúnek, 2016), land use (Gates et al., 2011), and soil-water use by vegetation (Zhang et al., 2018). Several studies have emphasized the importance of diffuse infiltration and percolation through loess and other fine-grained soils as the dominant recharge process (Deng et al., 2015; Dafny and Šimúnek, 2016; Huang et al., 2017). However, some studies suggest other recharge processes, such as preferential flow through the unsaturated zone or infiltration through stream valley sediments may be important (Lin and Wei, 2006; Gates et al., 2011, 2014). The present study investigates recharge processes through a loess-mantled landscape in western Tennessee using hydrologic tracers in precipitation, soil, and groundwater along with water balance to assess mechanisms and magnitudes of recharge. The results emphasize the varying roles of multiple recharge processes and pathways beneath regions with complex surficial

* Corresponding author.
E-mail addresses: dlarsen@memphis.edu (D. Larsen), johnbursi@gmail.com (J. Bursi), bwaldron@memphis.edu (B. Waldron), sschfrnc@memphis.edu (S. Schoefernacker), jeason@memphis.edu (J. Eason).

https://doi.org/10.1016/j.ejrh.2020.100667
Received 29 July 2019; Received in revised form 20 January 2020; Accepted 21 January 2020
Available online 10 February 2020

stratigraphy, topography, and land-use history.

The Memphis aquifer is a major source of water for municipal and industrial supplies in the northern Mississippi embayment (ME) of the central U.S. (Brahana and Broshears, 2001). Previous research suggests that much of the recharge to the unconsolidated sand of the Memphis aquifer in western Tennessee occurs within the exposure belt of the aquifer (Parks and Carmichael, 1990; Brahana and Broshears, 2001); however, field–based assessment of recharge rates and mechanisms are lacking. Recent mapping studies indicate that recharge to the aquifer could be impeded by Quaternary loess and underlying paleosols on upland surfaces in the exposure belt of the Memphis aquifer in western Tennessee (Larsen and Brock, 2014). Despite the aquifer's regional importance, little is known regarding recharge processes in the unconfined region. Similar aquifers in unconsolidated sand with overlying loess or other fine-grained soils exist throughout the North American Midwest and Gulf Coast regions (Gates et al., 2014; Nolan et al., 2007) as well as other parts of the world (Dawes et al., 2012; Dafny and Šimúnek, 2016) and may have similar processes affecting recharge rates and pathways.

This present study focuses on evaluating recharge processes in a small watershed in the unconfined region of the Memphis aquifer in western Tennessee. The main objectives are to ascertain rates and pathways of groundwater recharge using meteorological and hydrologic measurements, geochemistry, and both environmental and applied tracer data. These data are used to constrain soil moisture conditions, hydrologic balance in the upland watershed, and chemical signatures of soil and surface waters as well as groundwater. Recharge pathways are addressed using an applied tracer (bromide – Br^-), and tritium (^3H) and sulfur hexafluoride (SF_6) residence times.

1.1. Previous work

Western Tennessee is mantled by 0–15 m of middle to upper Pleistocene loess overlying 0–30 m of Pliocene and Pleistocene fluvial terrace deposits and as much as 1000 m of Cretaceous and Paleogene sand, silt, clay and coal representing coastal plain and marine deposits (Moore and Brown, 1969; Russell and Parks, 1975). The loess includes as many as four distinct units separated by paleosols (Rodbell et al., 1997; Grimley et al., 2009; Pigati et al., 2014). The underlying fluvial-terrace deposits are comprised primarily of sand and gravel (Van Arsdale et al., 2008), but also commonly have paleosol development within fine-grained sediments in the upper meter (Larsen and Brock, 2014). The fluvial-terrace deposits disconformably overlie Cretaceous and Paleogene sediments comprising alternating sand-rich aquifer and silt- and clay-rich confining units that dip gently to the northwest at $< 1^\circ$ (Moore and Brown, 1969; Brahana and Broshears, 2001). Late Pleistocene and Holocene alluvium, comprised of sand and gravel overlain by sandy silt, partially fill modern stream valleys (Carmichael et al., 2018; Grimley et al., 2009).

The Memphis aquifer consists of the Eocene Memphis Sand, which varies from coarse- to fine-grained unconsolidated sand with interbedded silt and clay (Moore and Brown, 1969; Parks and Carmichael, 1990; Lumsden et al., 2009; Larsen and Brock, 2014). The Memphis aquifer is regionally confined by clay and silt strata in the upper Claiborne confining unit in westernmost Tennessee, but is unconfined to the east of the confined region, due to the shallow northwestern dip of ME strata and erosional removal of upper Claiborne strata (Russell and Parks, 1975; Parks and Carmichael, 1990). These conditions result in a ~50-km wide belt of unconfined Memphis Sand to the east of the confined region, where the sand is exposed mainly in upland stream valleys, but overlain by 3–5 m of Pliocene(?) fluvial-terrace deposits and Pleistocene loess beneath the upland surfaces (Larsen and Brock, 2014). The upper few meters of the Memphis Sand commonly have paleosol development with extensive accumulated clay (Larsen and Brock, 2014). Parks and Carmichael (1990) suggested that groundwater recharge results from infiltration of precipitation in the outcrop region of the Memphis Sand, but little is known regarding the details of the process. Current information indicates that recharge rates of the Memphis aquifer vary spatially across the region (Bailey, 1993; Brahana and Broshears, 2001) and, in some places, include leakage mechanisms through the overlying upper Claiborne confining unit (Parks, 1990; Bradley, 1991; Brahana and Broshears, 2001; Larsen et al., 2003, 2013; Gentry et al., 2006).

Groundwater elevation in the Memphis aquifer within the unconfined region in Haywood County, Tennessee (well Ha:H-007) varied between 0.3 and 1.0 m per year between 2003 and 2012 (United States Geological Survey, 2015), less than annual variations (typically between 2–3 m) within the confined Memphis aquifer in Shelby County during the same time period (Kingsbury, 2018). These data suggest recharge of the Memphis aquifer in both unconfined and confined regions, with more recharge in Shelby County where the pumping stress is focused (Kingsbury, 2018).

Water balance is commonly used to estimate recharge in humid, temperate regions (Scanlon et al., 2002). The soil-water balance equation (Rushton and Ward, 1979; Scanlon et al., 2002) is used to estimate recharge for a time period, Δt:

$$R = R_I + R_{sw} = P - ET - Q_{sw} + CR + \Delta S \quad (1)$$

Where R is total recharge, R_I is recharge due to soil infiltration, R_{SW} is recharge from seepage of surface water, P is precipitation, ET is evapotranspiration, Q_{SW} is surface water runoff, CR is capillary rise, and ΔS is change in soil moisture. This method has been implemented in humid regions (Sophocleus and Perry, 1985; Steenhuis et al., 1985; Wu et al., 1996), with limitations that include the accuracy of the water-balance flux measurements (Sophocleous, 1991) and characterization of the soil moisture and climatic variability in a watershed (Dingman, 2002).

Chloride mass balance (CMB) has been applied in semi-arid to humid regions to estimate recharge through loess and other fine-grained surface soils (Allison and Hughes, 1983; Macfarlane et al., 2000; Russo et al., 2003; Nolan et al., 2007; Gates et al., 2011; Huang et al., 2017) This method requires measurement of the precipitation per unit watershed area, the average chloride concentrations of precipitation (and dry deposition), and the average chloride concentration throughout the vadose zone or the

uppermost saturated zone (Allison and Hughes, 1978; Sharma and Hughes, 1985). Limitations to the CMB method include non-steady state chloride mass flux, difficulty quantifying runoff-sourced chloride, and preferential recharge through macropores (Wood, 1999). Because runoff may be significant in small (<10 km^2) upland watersheds in humid regions, the CMB equation was modified to include the quantity of chloride in discharge per unit watershed area (Gates et al., 2011):

$$R = \frac{P \times C_{Cl^- precip} - Q_{sw} \times C_{Cl^- runoff}}{C_{Cl^- recharge}} \quad (2)$$

Where R, P and Q_{sw} are as defined in Eq. 1, $C_{Cl^- precip}$ is the chloride content in P, $C_{Cl^- runoff}$ is the chloride content in Q_{sw}, and $C_{Cl^- recharge}$ is the chloride content in R.

Isotopic and anthropogenic chemical tracers can also be used to assess recharge rates (Scanlon et al., 2002). Applications include environmental approaches using radioactive isotopes (tritium, ^3H) (Solomon and Cook, 2000) or anthropogenic chemicals (chlorofluorocarbons or sulfur hexafluoride, SF_6) (Busenberg and Plummer, 2000) with known atmospheric source and residence time histories, as well as applied tracers, such as dyes and conservative ions (such as Br^-). An advantage of tracers is that they can track recharge from variation sources and of different residence times (Cook and Böhlke, 2000).

1.2. Site description

The Pinecrest study area is in the rural uplands of western Tennessee (Fig. 1), approximately 80 km east of Memphis. With almost 25 percent of western Tennessee acting as a recharge zone to the Memphis aquifer (Parks and Carmichael, 1990), the Pinecrest research site was chosen because of its central location in the exposure belt of the aquifer. The land use at the site is predominantly deciduous forest with cultivated grass fields on the upland surfaces. The Memphis area receives an average annual rainfall of 137 cm (National Weather Service, 2019). Although surrounded by agriculture land use, the Pinecrest site has not been farmed for approximately 40 years and no use of chlorinated pesticides is known. The surface soils in the area include a variety of silt loam Alfisols and Inceptisols on upland surfaces and silty sand Inceptisols and Entisols along the valley margins and valley floor (Flowers, 1964). The underlying geologic units on the uplands include 1–3 meters of loess, 1–2 meters of Pliocene(?) fluvial terrace deposits with paleosol development, and the Memphis Sand with paleosol development in the upper 1–3 meters (Larsen and Brock, 2014). Quaternary alluvium locally fills upland valleys and transitions down-gradient into alluvial fan deposits that extend into the floodplain of perennial streams (Fig. 1).

Pinewood Creek (PWC) is a small stream that flows through the study area. It is ephemeral in the upper reaches near the instrumented hillslope (Fig. 1) and intermittent in the lower reach (near DPW, Fig. 1). The shoulder of the upland hillslope lies at approximately 162 m above sea level (asl), whereas the PWC watershed terminus is about 120 m asl in elevation where it discharges to the Wolf River (Fig. 1). Sets of lysimeters and soil tensiometers (LT clusters) installed at 0.5, 1.0, and 1.5 m were placed at four locations along a hillslope: shoulder slope (SS), back slope (BS), back slope gully floor (GF), and valley floor (VF) (Fig. 1). Three wells were installed in the watershed for monitoring groundwater level beneath the upland surface (SS 2 in. – SS2), valley floor (VFW), and down-gradient valley floor (DPW) locations (Table 1). Each well was instrumented with a Solinst pressure transducer. A fourth monitoring well at the shoulder slope location (SS 4 in. – SS4) is screened along its entire length, but was not utilized in the study. A Davis Wireless Vantage Vue weather station installed at the hill top recorded temperature, atmospheric pressure, wind speed and direction, and precipitation. A Parshall flume with a pressure transducer was installed in PWC adjacent to the instrumented hillslope (Fig. 1) to calculate stream discharge in the ephemeral reach (e.g., Kilpatrick and Schneider, 1983). The transducers and weather station were synchronized and recorded measurements at 15-minute intervals.

2. Methods

Initial investigation of recharge on the upland surfaces involved drilling a vadose-zone borehole by hollow-stem auger in a grass field (at the weather station in Fig. 1) to a total depth of 44 m, at which point drilling was terminated in a dense white clay. Core obtained from the borehole was used to determine site stratigraphy and measure vadose-zone water content and chloride concentrations, for application of vadose-zone CMB method to estimate vertical recharge (Allison and Hughes, 1978, 1983; Sharma and Hughes, 1985; Deng et al., 2015; Huang et al., 2017). To evaluate recharge processes in the watershed, water-balance parameter measurements (Eq. (1)) were conducted in the study area from March 2014 to February 2015. Soil moisture, groundwater level, and groundwater geochemistry were monitored for a year. Three monitoring wells, a production well (pool well, Table 1), swimming pool water, and the stream water at the site were sampled for geochemistry in August 2014, along with ^3H and SF_6 in two of the monitoring wells. Tritium and SF_6 are useful tracers for determining subsurface residence time of waters as much as 60 years old (e.g., Wilson and Mackay, 1993; Cook and Böhlke, 2000). A NaBr applied tracer study was also completed along the hill slope to assess the short-term recharge rate and pathway of groundwater movement.

2.1. Field methods

The vadose-zone borehole was drilled dry with a 10-cm inner-diameter hollow-stem auger assembly. The individual drilling tubes were 152-cm long and fitted with two 76-cm long polycarbonate sleeves to eliminate moisture loss from the sampled sediment. Sample handling and analysis are described in Larsen and Waldron (2020 – accompanying MethodX paper)

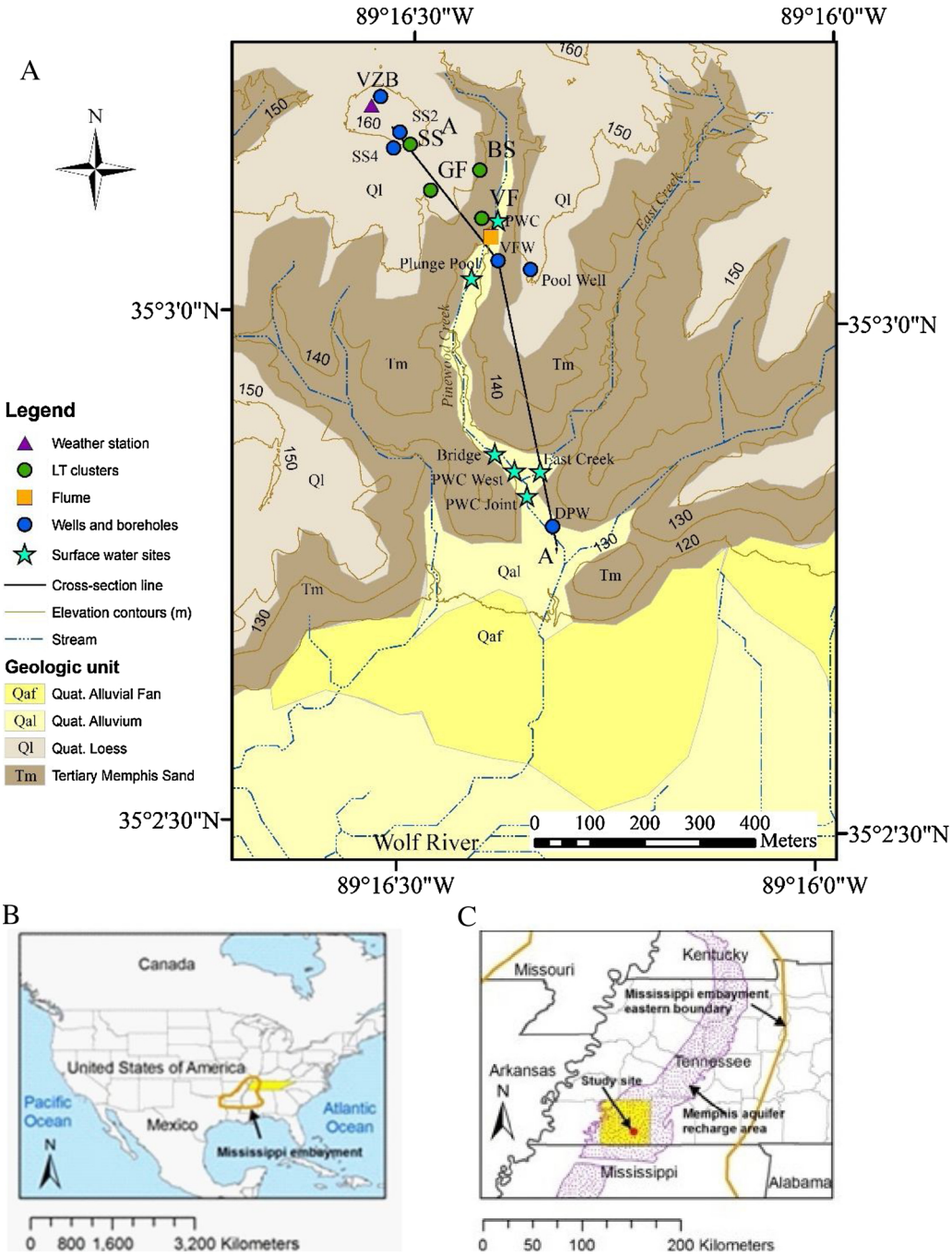

Fig. 1. A. Map of Pinecrest research site, Fayette County, Tennessee. Locations of LT clusters, wells, flume, weather station, and surface water sampling sites are shown relative to topography and surface geologic units (geology from Brock, 2012). Inset maps show the location of the study area in (B) the south-central US and (C) western Tennessee, respectively. Quat., Quaternary; BS, backslope; GF, gully floor; SS, shoulder slope; VF, valley floor; DPW, drive-point well; SS2, 2-inch diameter well at shoulder slope; SS4, 4-inch diameter well at shoulder slope; VFW, valley-floor well; PWC, Pinewood Creek. Cross-section line A-A' shown in Fig. 11. Contour interval is 10 m.

Water balance and hydrochemical data collection were made on a bi-weekly schedule from March 2014 to February 2015 (Bursi, 2015). Bi-weekly field tasks included measuring water volume in lysimeters and pressure in tensiometers, downloading data from the weather station, and inspecting the flume to ensure proper function and flow through the device. Monthly tasks include measuring groundwater levels, sampling lysimeter and stream water for geochemical analyses, and downloading transducer data.

The flume transducer data were compensated with the barometric pressure data from the weather station. For each discharge event, a baseline was defined based on the transducer pressure prior to the event. This baseline was then applied throughout the

Table 1
Well construction and design.

Well Name	Construction Material	Diameter, I.D. (cm)	Depth (m)	Screened Depth Interval (m)	T.O.C. Elevation (m)
SS2	PVC	5	70	52-70	163
SS4	PVC	10	70	0-70	162
VFW	PVC	10	35	32-35	143
DPW	Steel	5	4	3-4	121
Pool Well	PVC	10	65.5	62.5-65.5	150

I.D. – inner diameter.
T.O.C. - top of casing.

discharge event. Any measured pressure that surpassed this baseline was evidence of discharge. Data gaps occurred from July 3–17, 2014. Precipitation events during this time were compared to similar events based on precipitation quantity and intensity. Discharge was then estimated for that period based on a linear stream response to similar events.

The tensiometers were checked to ensure they had not run dry, which produces a false zero measurement. If the tensiometer still had water during a site visit, the measurement was recorded, in centibars (cb), and then refilled with deionized water. Tensiometer gauges were removed in late November 2014 to avoid freezing. Lysimeter water was purged into 2 L amber bottles with a transfer cap using a vacuum hand pump. Tubing and bottles were triple rinsed with deionized water after every use.

Monthly static groundwater level measurements were made using a Solinst water level meter. Measured groundwater elevations and barometric pressure (from the weather station) were used to correct transducer data obtained from wells. Abrupt rise or fall in the pressure transducer data resulted from inconsistent pressure transducer position in the well and error with the barometric compensation.

Field geochemical measurements include pH, temperature, dissolved oxygen, and specific conductance. Raw and filtered, acidified water samples were obtained at the sampling sites if sufficient water existed after the field parameters were taken. Filtered and acidified samples were obtained after passing through a 0.45 μm microcellulose filter and preserved with concentrated nitric acid (HNO_3) to achieve a 1 % nitric acid solution. All water samples were stored on ice in a cooler and returned to the water lab at the University of Memphis for analysis of alkalinity and major dissolved cations and anions.

In August 2014, the monitoring wells and PWC, at locations near the DPW, were sampled for field geochemical measurements and laboratory analysis. Grab samples of surface, swimming pool, and subsurface water were obtained and analyzed using the same procedures as described above for the lysimeter waters, except that total alkalinity was performed in the field instead of the lab. Water from the pool well was obtained from a spigot adjacent to the well. Water from the DPW was obtained by bailing three borehole volumes from the well. Water samples from the deep wells (SS2 and VFW) were obtained by low-flow pumping from depth using a submersible turbine pump, and monitored using a YSI-6600 multi-parameter probe to assess stabilization of the field geochemical measurements. Once the field geochemical measurements stabilized, final field geochemical measurements were recorded, and samples were taken and stored in the same manner as those from grab samples. Field geochemical measurements were also collected from the DPW and pool well and samples returned to the lab for analysis. Duplicate samples, field blanks, and equipment blanks were obtained to assess the quality and reproducibility of chemical data.

Groundwater samples for ^3H and SF_6 from the SS2 and VFW wells were collected in one-liter, air-tight amber bottles. The sample bottles were primed with continuous flow for five minutes and then filled and sealed with electrical tape over the cap to prevent air from entering the sample. Samples for ^3H and SF_6 were analyzed at the University of Utah Dissolved and Noble Gas Laboratory.

A tracer injection was performed to assess rate and pathway of infiltration from the hillslope LT cluster (BS, Fig. 1) to the water table on November 11, 2014. Sixty liters of 500 ppm NaBr solution were injected through a 3-m neutron probe borehole at the BS hillslope location, which was determined by soil moisture studies to be the most effective location for recharge (see Section 3.2). Samples were periodically taken following injection from the DPW, SS 4 in., and VFW locations, and at surface water locations from the stream just north of DPW and another slightly to the south of VFW (Fig. 1). The wells were sampled using dedicated bailers and string for each well. Surface water was sampled by taking grab samples from water sources. Bromide was initially sampled twice a week, then once a week from November 26 to December 22, 2014, and then bi-weekly from January 5 to February 25, 2015. After February 25, 2015, monthly sampling continued until July 2015.

Three or more slug tests were performed on the DPW and SS2 wells. Water levels were measured using a Solinst M10 levelogger transducer with a 1-second measurement interval and manual measurements with electric water level tape. Five to 10 gallons of water were used to displace the static water level, depending on the well bore volume. The data were analyzed using the Bouwer and Rice method (Bouwer and Rice, 1976).

2.2. Laboratory methods

Grain-size analysis was performed on samples from neutron probe and monitoring well boreholes using a modified soil analysis method (Gee and Bauder, 1986). The grain-size data were used to estimate hydraulic conductivity using the method of Shepherd (1989).

Within a day of collection, raw samples were filtered and analyzed in duplicate for total alkalinity using a Hach digital titration

system. Within a day of sample acquisition, major and minor anions (F^-, Cl^-, NO_2^-, Br^-, NO_3^-, PO_4^{3-}, and SO_4^{2-}) were analyzed from lab-filtered subsamples using a Dionex DX-120 ion chromatography (IC) unit. The Br^- tracer samples were filtered and run on the IC in a similar manner. Six major and minor cations (Na^+, Ca^{2+}, K^+, Mg^{2+}, Mn^{2+}, and Fe^{2+}), were analyzed from the filtered, acidified samples using a Varian FS220 flame atomic absorption (AA) unit. The precision of F^-, Cl^-, SO_4^{2-}, and all cations is 10 % or less using an internal lab standard. The accuracy of the anion analyses had a larger range, within 0.1 %–27 % of published values for the Dionex seven anion standard. The average charge balance error for all samples was −3.1 % with a range of −41.7–39.6%. The large departures from zero can be attributed to many variables. Most rain samples contained insect residue and a few contained bird feces. The installation of a screen over the gauge and barb deterrents helped the issue, but never eliminated it. Though the precipitation samples were filtered, the dissolved constituents from these contaminants were not eliminated. The stream waters also contained decaying organic matter such as leaf litter or insects.

Tritium activity was determined using the helium in-growth method (Clarke et al., 1976; Bayer et al., 1989). The practical detection limit for the helium in-growth method is 0.05 TU (Solomon and Cook, 2000). Under typical conditions, the laboratory error for Tritium analysis ranges from approximately ± 10 % at 1 TU to ± 70 % at the detection limit (Schlosser et al., 1988). Sulfur hexafluoride was analyzed by GC-ECD techniques to a precision of 1–3 % at concentrations in excess of 1.0 fg/L to a maximum reporting level of 3.0 pg/L (Wanninkhof and Ledwell, 1991; Law et al., 1994). This precision and detection limit permit groundwater dating applications from about 1970 to the present (Busenberg and Plummer, 2000). The precision of groundwater age calculated from SF_6 data depends on the analytical errors (generally ± 5 %), error in the estimated recharge temperature (±2 °C = 1–3 years age difference), and error due to residence time in the unsaturated zone (as much as 8–12 years for unsaturated zone thickness of 30 m) (Busenberg and Plummer, 2000). The tritium and SF_6 data were modeled using USGS TracerLPM (Jurgens et al., 2012) to examine the primary flow regime: Piston Flow model - PFM, Exponential Piston-Flow model - EPM, and Exponential Mixing model - EMM.

2.3. Data analysis

A water balance estimate for the upper part of the PWC watershed was calculated from March 1, 2014 to February 28, 2015, using Eq. 1, data from the Pinecrest weather station and nearby weather stations, and discharge data from the flume. Weather station data were not available from 10/15/15 – 10/29/15 and 12/23/14 – 1/7/15. Data from these time periods were obtained from two different sources. Daily averages for precipitation and temperature were recorded from a National Oceanic and Atmospheric Administration (NOAA, 2015) land-based weather station at Ames Plantation, approximately 8.4 km northeast of Pinecrest. Humidity, wind speed, and barometric pressure were obtained from a personal weather station in Rossville, Tennessee, approximately 26 km west of Pinecrest. Daily ET data were calculated from the Pinecrest weather station data, except for solar radiation. Solar radiation data were averaged from measurements at two nearby weather stations (Winborn, Mississippi, 48 km south, and Chickasaw State Park, Tennessee, 53 km northeast) (WU, 2015). These data were combined with the Pinecrest weather station data and applied to the Penman-Monteith equation (Allen et al., 2005; Zotarelli et al., 2009) to calculate daily ET.

The saturated-zone CMB recharge was calculated using Eq. 2 with the mean chloride concentration of precipitation, saturated-zone water and runoff at the flume location as well as the measured precipitation and discharge in the upper PWC watershed from the 2014-15 data.

The vadose-zone CMB recharge estimate was calculated using Eq. 2 with mean chloride concentration in sediments from the vadose-zone borehole and estimates of mean annual precipitation and chloride concentration in precipitation. Loss of chloride from discharge in runoff is not incorporated into the calculation because the vadose-zone borehole was drilled on a flat ridgeline where runoff is considered negligible; hence, precipitation is the sole source of chloride to the system. A National Atmospheric Deposition Program (NADP) station, TN14 (50 km north of Pinecrest), has recorded chloride wet-fall concentrations since 1984 yielding a mean precipitation-weighted annual chloride concentration of 0.17 mg/l (http://nadp.sws.uiuc.edu/sites/siteinfo.asp?net=NTN&id=TN14).

Hydraulic conductivity for the Memphis aquifer was estimated using grain-size analysis from samples taken from the neutron probe borings at locations BS, GF, and DPW and push-core samples from VFW and SS2 (Appendix B). The hydraulic conductivity was calculated using the Sheppard method (Fetter, 2001) applied to 5 boring samples and 12 push core samples. Hydraulic gradients and hydraulic conductivity were used to estimate an arrival time:

$$Travel\ Time = \frac{L(n_e)}{(q')} \tag{3}$$

Where L is flow length (m); q' is specific discharge (m/d); n_e is effective porosity.

3. Results

3.1. Vadose-zone borehole

The sediment recovered from the hollow-stem auger records 3.9 m of sandy silt (Quaternary loess), 2.1 m of fine- to medium-grained sand with sparse iron-oxide cemented pebbles (Pliocene(?) fluvial-terrace deposits), and 30.6 m of fine- to medium-grained and fine to very coarse-grained sand (Eocene Memphis Sand) with thin intervals (< 20 cm) of clayey sand, followed by 0.4 m of white clay (Fig. 2). The basal contact of the loess is gradational over 0.4 m with the sand and gravel deposits. Paleosol development is

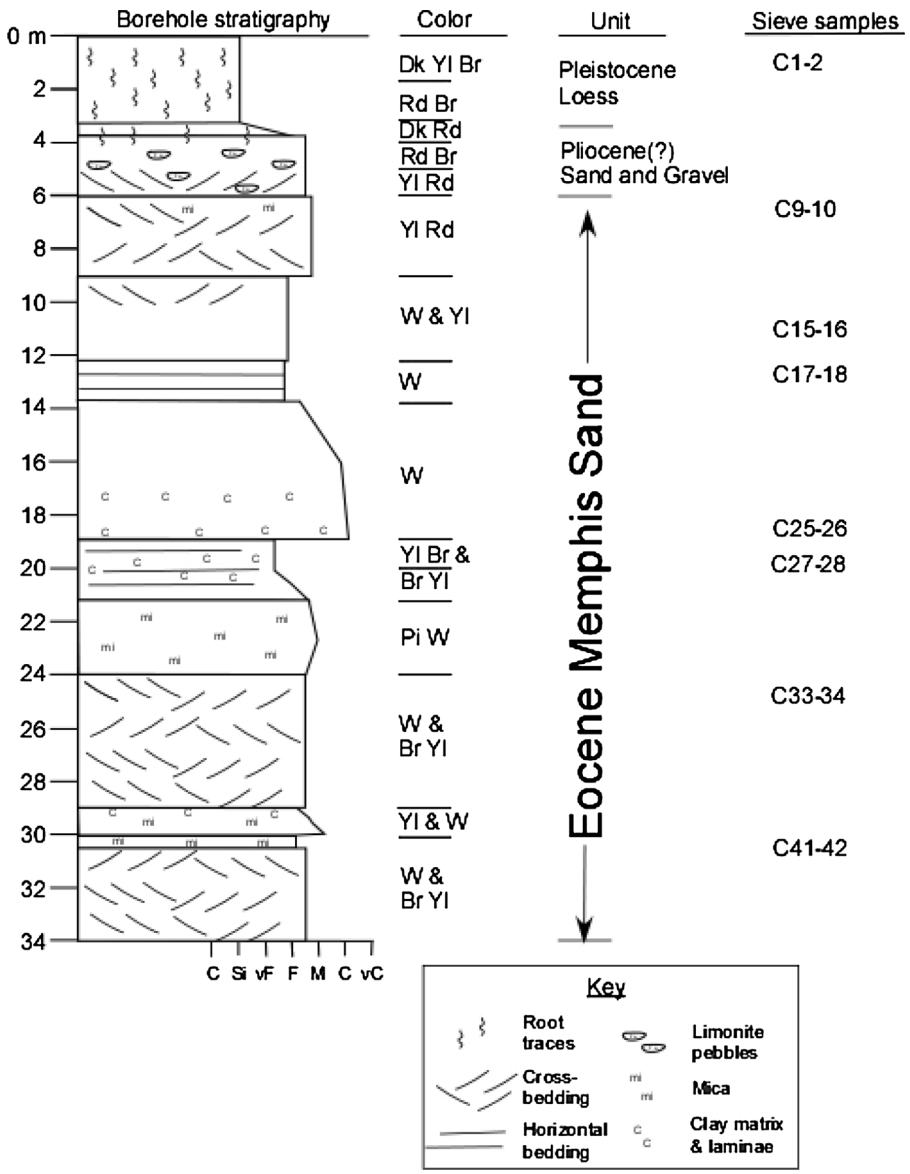

Fig. 2. Stratigraphic column for Pinecrest vadose-zone borehole showing lithology, Munsell color, geologic units, and sieve samples. Color abbreviations: Dk Yl Br, 10YR 3/6 (dark yellowish brown); Rd Br, 5YR 4/4 (reddish brown); Dk Rd, 2.5YR 3/6 (dark red); Yl Rd, 5YR 5/8 (yellowish red); W, 2.5YR 8/1 (white); Yl, 2.5YR 8/1 (yellow); Yl Br, 7.5 YR 5/8 (yellowish brown); Br Yl, 10YR 6/6 (brownish yellow); Pi W, 2.5 YR 8/2 (pinkish white) (For interpretation of the references to colour in this figure legend, the reader is referred to the web version of this article).

evident in the sand and gravel, similar to that observed in surface exposures by Brock (2012). The sand in the underlying Memphis Sand is composed almost entirely of quartz with conspicuous mica being present in several intervals (Fig. 2), similar to petrographic and mineralogical observations (Lumsden et al., 2009; Larsen and Brock, 2014).

Water content shows a gradual decrease with depth from 16.75 % at 2.30 m to 3.13 % at 10.0 m (Fig. 3). The relatively higher moisture contents at depths of 12.6–13.1 m, 20.1–20.7 m, and 30.5–31.0 m correspond to the top of fine-grained intervals (Fig. 2). Chloride concentration generally increases with depth with prominent high concentrations at 17.0 m, 26.5 m, and 27.9 m depth. Peak chloride concentrations do not correspond to variations in water content or to stratigraphic changes.

3.2. Physical hydrology

Daily discharge data show flow in Pinewood Creek only during prolonged or intense rainfall events (Fig. 4).

Biweekly lysimeter volumes at the 1.5 m depth are greatest during the wet periods of the year, but lower during the summer and fall except for the SS location (Fig. 5A). The biweekly tensiometer pressure shows less consistent relationship to seasonal precipitation

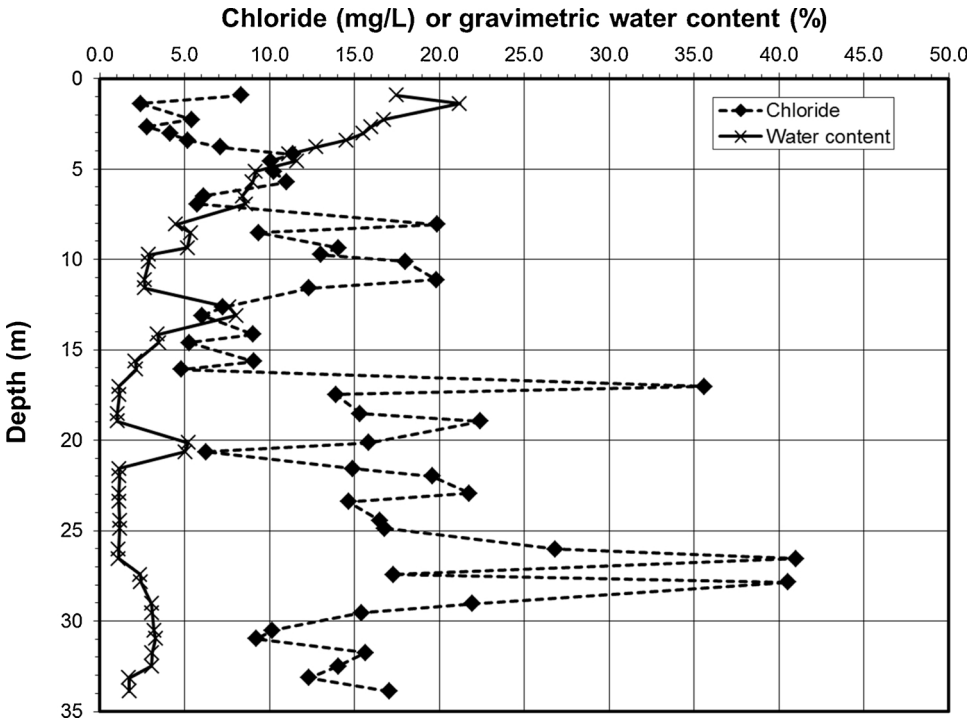

Fig. 3. Water content (gravimetric) and chloride concentration of Pinecrest vadose-zone borehole samples versus depth.

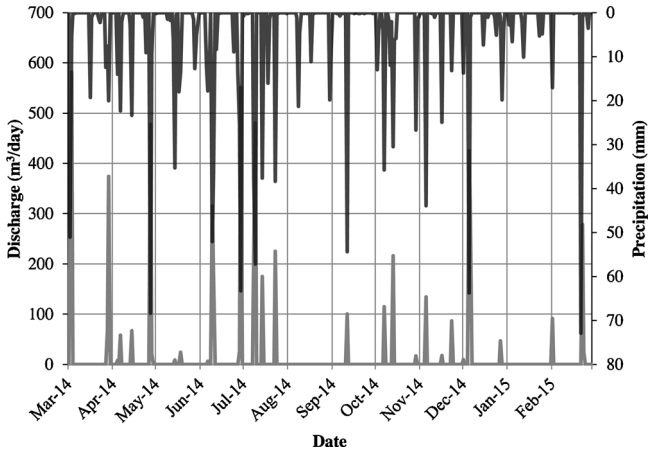

Fig. 4. Daily discharge measurements (light gray) in Pinewood Creek and precipitation totals (dark gray) for the observation year, March 2014 – February 2015. Occasional freeze/thaw occurred in early January and persisted until the end of February 2015.

(Fig. 5B), although soil tension increases during the summer and fall at the BS and VF locations.

Average daily groundwater elevation for the SS2 and VFW wells varies by 0.25 and 0.15 m, respectively, during the year, with the highest levels observed during fall and early winter months (Fig. 6). Groundwater elevation at the DPW well is highest during the spring, early summer and winter when flow is observed in the lower reach of Pinewood Creek, but falls to the level of the SS well during the late summer and fall.

3.3. Geochemical data

Precipitation samples obtained during the year vary greatly in pH, specific conductance, alkalinity, and solute composition (Table 2, Appendix A). Assuming that samples obtained during spring and summer show the greatest impact of insects, birds, and evaporation, the precipitation samples from the late fall and winter months likely provide the best representation of the precipitation composition. The pH of precipitation obtained from November 2014, through February 2015, range from 4.61 to 5.64, with pH from spring through early fall, 2014, ranging from 3.90 to 6.61. Specific conductance from November 2014, to February 2015, ranged from

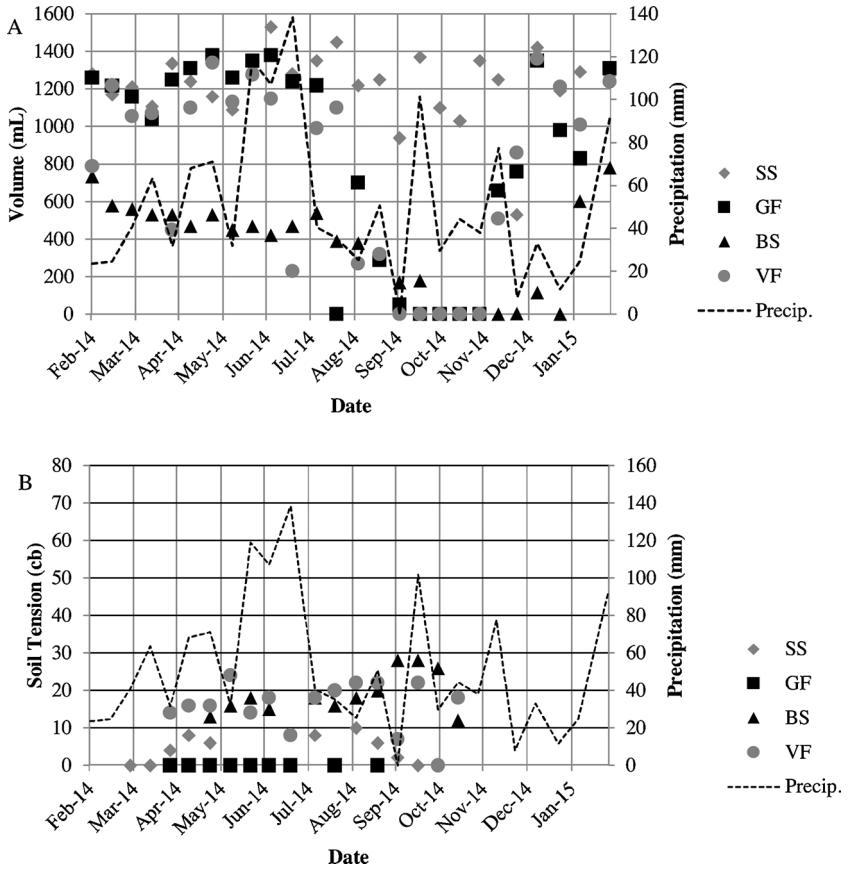

Fig. 5. Data from (A) lysimeters and (B) tensiometers installed at 1.5 m depth for the observation year. Lysimeter volumes (ml) and tensiometer pressures (cb) are plotted with total precipitation (mm) during each 2-week observation period. Tensiometers were removed during November through February when freezing temperature might occur. Measurement locations are illustrated in Fig. 1.

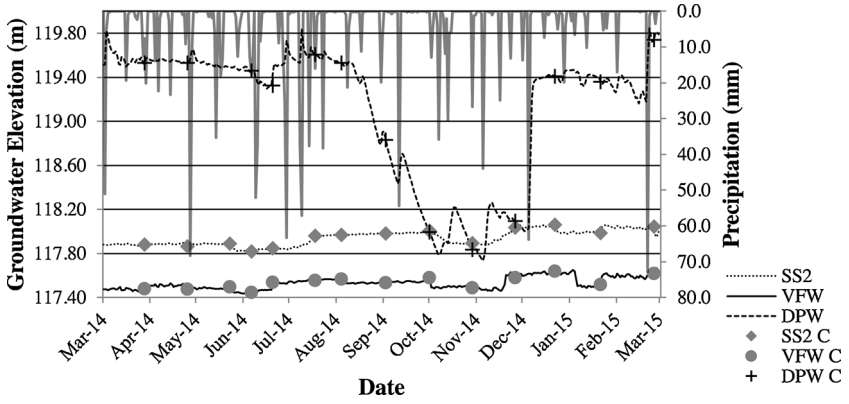

Fig. 6. Daily average groundwater elevation (m asl) plotted with daily precipitation totals for the observation year. "C" data series represent the manual water level measurements.

9.07–13.3 µS, whereas values from spring 2014 to early fall 2014 range from 4.55–1480 µS. The lowest specific conductance was observed on May 23 after a week of light rain on May 12 through 19 and the highest specific conductance was observed on July 18 two days after an intense rainfall event.

Samples taken from surface water sources for chemical analysis were obtained when flow was observed in the creeks. Water was flowing in PWC during only two monitoring events during the 20-14-2015 observation year. Other samples were taken at East Creek and PWC Joint locations, and the swimming pool during the deep well sampling event in August 2014 (Fig. 1). East Creek and PWC Joint are similar in their major ion composition (Fig. 7). One of the samples obtained at the upstream PWC sampling location (2/25/

Table 2
Precipitation and surface water sample field data.

Sample Name	Sample Date	Field Temp. (°C)	Field pH	Field S.C. (μS)	Field D.O. (mg/L)	Lab Alk. (mg/L)
Rain 3/14	3/14/2014	14.5	3.90	23.8	nd	bd
Rain 4/11	4/11/2014	24.3	6.51	54.4	nd	24.4
Rain 5/23	5/23/2014	31.5	6.45	4.55	nd	0.488
Rain 7/18	7/18/2014	18.8	5.42	1480	nd	3.66
Rain 9/17	9/17/2014	30.0	4.06	38.8	nd	bd
Rain 10/15	10/15/2014	19.3	6.32	16.9	nd	1.22
Rain 11/12	11/12/2014	7.50	4.61	9.07	nd	1.46
Rain 12/9	12/9/2014	11.2	5.28	8.54	nd	3.66
Rain 1/5	1/5/2015	2.90	5.06	13.3	nd	1.71
Rain 2/4	2/4/2015	9.70	5.64	12.9	nd	0.732
PWC 3/28	3/28/2014	24.8	6.32	94.4	nd	20.7
Pool Water 8/4	8/4/2014	14.9	7.15	218	nd	57.4
PWC East 8/6	8/6/2014	21.2	7.01	52.8	8.00	21.0
PWC West 8/6	8/6/2014	21.1	6.88	64.9	7.00	25.2
PWC Joint 8/6	8/6/2014	21.3	6.83	58.4	7.60	22.4
PWC Bridge 11/19	11/19/2014	12.5	6.96	72.5	7.10	nd
Plunge Pool 11/19	11/19/2014	12.3	7.66	143	8.40	nd
PWC 2/28	2/25/2015	16.1	7.04	52.3	nd	18.2

S.C. – specific conductance; D.O. – dissolved oxygen; Alk. – alkalinity.
nd - no data.
bd – below detection.

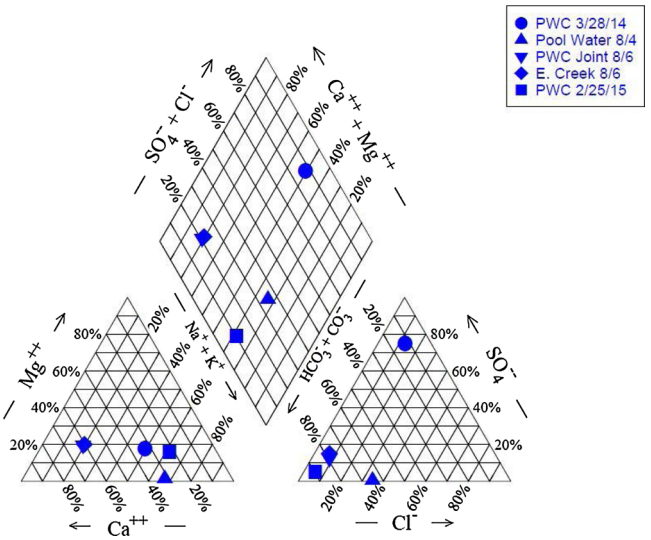

Fig. 7. Piper diagram of surface water samples.

15) is similar to, but more sodium rich, than the East Creek and PWC Joint samples. In contrast, the upstream PWC from 3/28/14 is more sulfate- and chloride-rich, but otherwise similar to the 2015 upstream PWC sample in regard to the major ion composition. The upstream PWC sample from 3/28/14, however, was warmer, slightly more acidic and had nearly the highest specific conductance (94 μS) than all surface water samples, suggesting that it may have derived from a mixed water source.

Due to the large number of soil-water samples taken from the lysimeters for geochemical analysis (Appendix Tables A1 and A2), a representative sample from each meteorological season is plotted in Fig. 8 to illustrate the variability of soil moisture composition during the year. Samples from only the 1.5-m depth are shown to reflect water compositions below the influence of root action by plants. All of the soil waters are sodium-sulfate-bicarbonate waters. Chloride concentrations in soil water are enriched relative to rain water by a factor of 2–4. In contrast, sodium, sulfate, and alkalinity are enriched in soil water relative to rain water by a factor of approximately 10–200, indicating a soil-based source for these ions. The soil water samples are enriched in sodium and sulfate in comparison to surface water samples, suggesting that soil water is not commonly a significant component of surface runoff in the creeks. Seasonal variations in soil water composition are most prominent in the GFL and BSL samples with sulfate-rich water dominant during the spring and bicarbonate-rich water dominant during the summer. The fall and winter soil-water compositions trend back toward sulfate-rich compositions, suggesting a yearly cycle in soil-water composition (Fig. 8).

Groundwater chemistry data from the August 2014 sampling event are tabulated in Table 3 and Appendix Table A2 and displayed

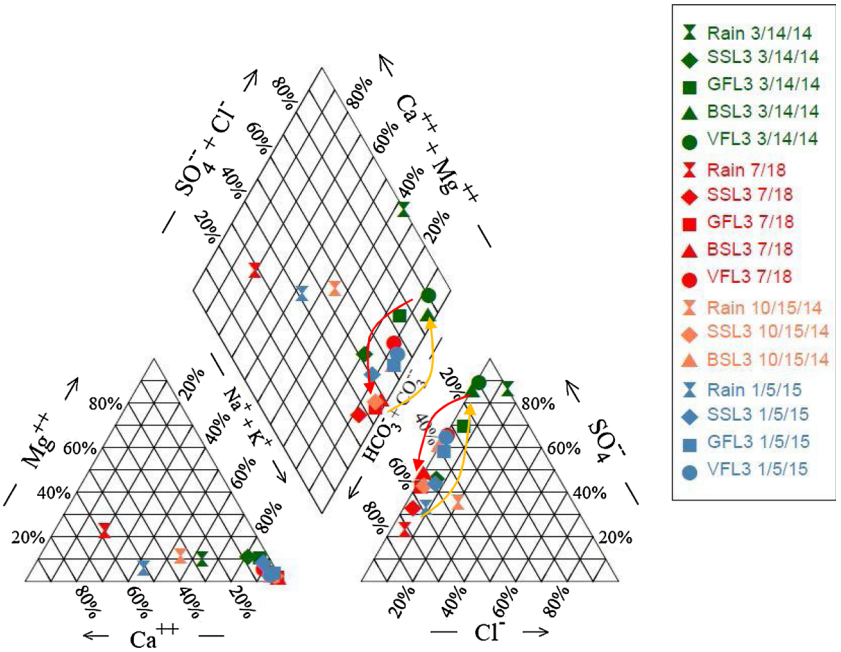

Fig. 8. Piper diagram of representative soil water samples from the 1.5 m lysimeters and precipitation. Symbol shape represents sampling location, whereas color represents season. Colored arrows show seasonal changes in water chemistry.

Table 3
Groundwater sample field data.

Sample Name	Sample Date	Field Temp. (°C)	Field pH	Field Eh (mV)	Field S.C. (µS)	Field D.O. (mg/L)	Field Alk. (mg/L)
VFW 8/4	8/4/2014	22.5	6.30	318	115	4.49	34.6
Pool Well 8/4	8/4/2014	16.8	5.98	478	29.6	7.60	10.8
DPW 8/6	8/6/2014	20.3	5.79	363	48.7	2.30	12.8
SS2 8/6	8/6/2014	24.4	5.34	469	37.6	5.70	10.4
DPW 11/19	11/19/2014	14.4	6.39	nd	67.2	7.90	nd
VFW 11/19	11/19/2014	15.5	6.99	nd	143	4.30	nd
SS2 11/19	11/19/2014	14.5	6.40	nd	121	8.30	nd

S.C. – specific conductance; D.O. – dissolved oxygen; Alk. – alkalinity.
nd - no data.

on Fig. 9. VFW, SS2, and the Pool well show similar mixed cation-HCO_3 chemical signatures, whereas DPW shows a slight increase in SO_4^{2-} and decrease in Cl- relative to the other groundwater samples. The DPW water is very similar in composition to surface water samples from East Creek and PWC joint, although NO_3- and Ca^{2+} are higher in the creek waters.

3.4. Tracer study

3.4.1. Applied tracer

During the tracer injection event on November 19, 2014, initial samples were taken from all locations that would be periodically sampled for presence of the Br^- tracer (Fig. 1) to ensure no significant Br^- existed previously at these locations. Bromide tracer was not found at concentrations above background until April 22, 2015, in a single sample at the VFW (Table 4).

3.4.2. Environmental tracers

Tritium results for the SS2 and VFW were 5.53 tritium units (TU) and 2.56 TU, respectively. Sulfur hexafluoride results were 0.64 parts per trillion per volume (pptv) for SS2 and 2.31 pptv for VFW. Lumped parameter modeling of the data show the best fit with a piston flow model (PFM) (Fig. 10).

3.5. Water balance

Precipitation, ET, and discharge data were averaged over the watershed area (1.189×10^5 m^2) to determine the water balance for the year. Total precipitation was 1433 mm and total ET, 920 mm. The measured discharge was 505 mm for the year. Applying these

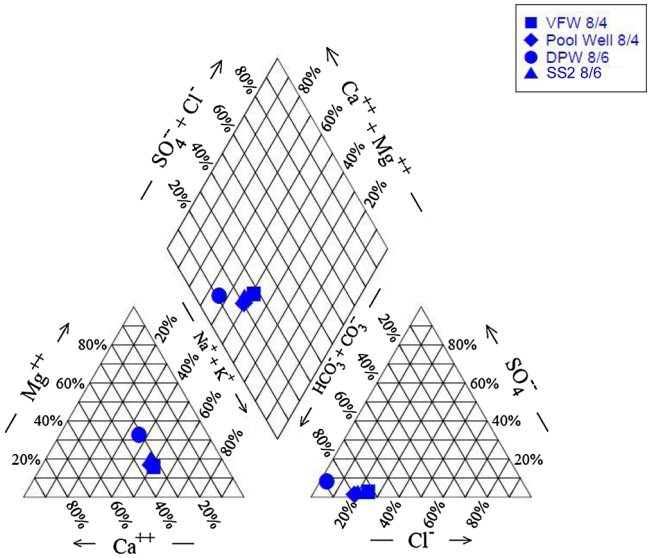

Fig. 9. Piper diagram of groundwater from the August 2014 sampling event.

Table 4
Bromide concentration of VFW sampling location.

Sample Name	Sample Date	Br^- (mg/L)
VFW 8/4	8/4/2014	0.02
VFW 11/19	11/19/2014	0.01
VFW 11/21	11/21/2014	0.02
VFW 11/26	11/26/2014	0.02
VFW 12/3	12/3/2014	0.01
VFW 12/9	12/9/2014	0.01
VFW 12/17	12/17/2014	0.01
VFW 12/22	12/22/2014	bd
VFW 1/5	1/5/2015	0.02
VFW 1/21	1/21/2015	0.02
VFW 2/4	2/4/2015	0.02
VFW 2/25	2/25/2015	0.02
VFW 3/20	3/20/2015	0.01
VFW 4/22	4/22/2015	2.44
VFW 4/29	4/29/2015	0.02
VFW 5/20	5/20/2015	0.02
VFW 6/17	6/17/2015	0.02
VFW 7/15	7/15/2015	0.02

bd-below detection.

data to water balance Eq. (1) and assuming no change in capillary rise or soil moisture, the recharge is 7.5 mm for the observation year. Assuming 5 % error, the water balance ranges from water-balance excess to deficit, indicating the sensitivity of the recharge estimate to errors in the comparatively larger magnitudes of precipitation and ET. Under most conditions with increased discharge or ET relative to a decrease in precipitation, the water balance yields a deficit.

3.6. Chloride mass balance

The vadose-zone CMB was used to estimate multi-year recharge at an upland hill top location. The mean vadose-zone chloride concentration, evaluated from 1.5 m (base of the root zone) to 34.0 m (Fig. 3), is 14.21 mg/L with a standard deviation of 8.58 mg/L. Using the mean regional precipitation rate of 137 cm/yr, the estimated recharge rate was 16.4 mm/yr with a one standard-deviation range of 10.2–41.3 mm/yr. Given that the water table was not reached during drilling and that low-permeability layers might limit redirect vertical flow through the vadose zone, the rate obtained must be considered as potential recharge (Rushton, 1988; de Vries and Simmers, 2002) and not as actual recharge.

The saturated zone CMB was used to estimate recharge from the 2014-15 observations at the Pinecrest site. Chloride analytical data are compromised in some cases by insect and bird residue, thus only data with calculated electrical balance of less than 20 % are used to calculate the mean concentration in precipitation. This results in mean chloride concentration in rainfall of 0.36 mg/L and

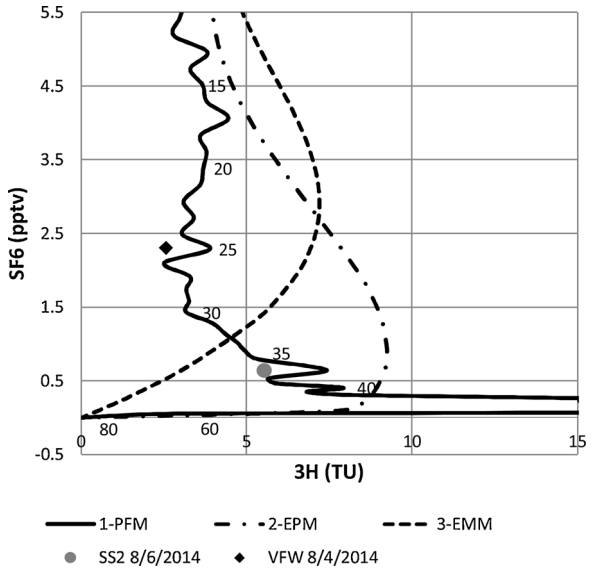

Fig. 10. Lump parameter models created for age-date results. The SF_6 loading curve in pptv is for the northern hemisphere (Jurgens et al., 2012). Tritium loading history in TU is from the Missouri River Basin (Michel, 2004). The ages in years are plotted for the PFM.

discharge of 1.0 mg/L. Using the measured precipitation and discharge data with the selected chloride concentrations for precipitation and runoff, and the chloride concentrations in the SS2 and pool wells (Appendix Table A2), recharge varies from 4.8–6.2 mm/yr. Propagation of 5 % errors in measured precipitation, discharge, and chemical analysis yield a wide variety of values, ranging from water balance excess to deficit.

3.7. Hydraulic conductivity

The arithmetic mean of 8 slug tests at the SS2 and DPW locations yields a hydraulic conductivity for the Memphis aquifer of 3.7 m/d (Appendix B). The arithmetic mean of hydraulic conductivity for the Memphis aquifer from grain-size analysis of 5 boring samples (BS, GF, and DPW) and 12 push core samples (VFW and SS2) is 4.0 m/d (Appendix B).

4. Discussion

4.1. Physical hydrology

The measured climatological data for the 2014–2015 observation period indicate conditions similar to regional values with the exception of higher calculated ET. The annual precipitation for the site was 143.2 cm, 5 % higher than the regional mean of 137 cm/yr. The maximum temperature for the year was 28 °C, the minimum was −8 °C and the mean was 14.6 °C. The normal yearly average from a nearby weather station is 14.7 °C (NOAA, 2015). The total ET was 920 mm/yr, somewhat higher than regional estimates of 710–800 mm/yr (Sanford and Selnick, 2012). Recent estimates of ET in urban watersheds in Jackson, Tennessee, 82 km north of Pinecrest, range from 703 mm/yr (Simco, 2018) to 834 mm/yr (Smith, 2019).

Discharge in PWC at the flume location is ephemeral with flow only occurring during or after major precipitation events (Fig. 4). During periods of the year in which long-duration (one or more days) weather-front precipitation events are common, the stream flows more often, likely fed by overland flow due to limited infiltration into saturated soil. An additional limitation to infiltration may occur during fall and winter when leaf litter covers the majority of the forest floor. During the drier months, discharge response to precipitation is more muted or non-existent. Along the downstream reaches of PWC, slightly upstream and downstream of the confluence with East Creek (Fig. 1), flow is more continuous, except during the late summer and early fall, as indicated by the decrease in water level at the DPW during this time. Seasonal seepage occurs along the lower reaches of PWC at the interface of sand and clay beds in the Memphis Sand and likely contributes to more continuous flow in the lower reaches of PWC.

Soil water data provided by the lysimeters and tensiometers show strong seasonal trends in moisture content, but are also influenced by soil texture. Lysimeter data show seasonal soil water storage in silt-rich soils, such as those at the SS and VFW locations, with lysimeters yielding more water during the wetter months and lesser volumes in the drier months (Fig. 5). The water volumes at the BS location are generally lower in all seasons compared to other locations, reflecting percolation through sandy surface soils. The tensiometer data show similar variations to those of the lysimeter volumes but have more dependence on soil type. Because the BS location continually yielded little water in lysimeters and shows high soil tension, infiltration is interpreted to occur at a higher rate along the hillslope locations, where sandier textures exist. The GF location shows low lysimeter volumes similar to the BS location, but the tensiometer data show low soil tension. The tensiometer data for the GF location appear to be compromised by instrument

malfunction.

The climatological and surface hydrology data at the Pinecrest site indicate that the observation year had weather conditions typical for the region. Higher precipitation and lower ET during the early winter through late spring create excess soil moisture available for drainage through soil (Flowers, 1964) to recharge groundwater storage. Retention of soil moisture in silt-rich soils observed on the upland surface (SS location) and alluvium in the valley floor (VF location) retard infiltration through the soil zone, resulting in overland flow and surface runoff during long duration precipitation events. Infiltration is more rapid in sandy soils (locations BS and GF) and where Memphis Sand and sandy alluvium crop out at the surface (location DPW).

4.2. Vertical recharge and recharge pathways

The vertical recharge rate below the soil zone in the upper part of the PWC watershed were determined using water balance, the CMB methods, and environmental tracers. The vadose-zone CMB method provides a long-term estimate for recharge of 16.4 mm/yr. If one assumed runoff impacts, water-balance data from 2014 to 2015 suggests that approximately 35 % of the precipitation becomes runoff. If 35 % of precipitation and associated chloride are removed from the total precipitation in the vadose-zone CMB calculation, the long-term recharge rate is 11 mm/yr. This recharge rate is of similar magnitude to the range of recharge rates of 4.8–6.2 mm/yr obtained for the 2014–2015 saturate-zone CMB recharge rate as well as the 7.7 mm/yr rate obtained from water balance. In theory and in practice, the unsaturated- and saturated-zone CMB methods do not typically provide similar values for recharge (Johnston, 1987a, b; Scanlon et al., 2002). The saturated-zone CMB method applies to larger spatial domains, in part due to lateral flow of groundwater (Wood and Sanford, 1995). Ideally, the chloride concentration from the vadose-zone chloride profile should have little variation with depth (Wood, 1999); however, notable spikes in chloride concentration are observed at 17, 27, and 28 m depth. The central United States is known to have experienced protracted periodic drought during the 1850 – 60 s, 1910s, 1930s, and 1950 – 60 s (Burnette and Stahle, 2013), which may have affected the short-term chloride concentration resulting in lower recharge rates.

The pathway of recharge to the Memphis aquifer in the upland valley was evaluated assuming rapid vertical migration of the column of Br^- solution during the applied tracer test at location BS and assessing the travel time to VFW. Specific discharge was calculated using the mean gradient from SS2 to VFW and the range of hydraulic conductivity of 3.7–4.0 m/d resulting in 0.66 to 0.72 m/d. Applying an effective porosity of 0.3 (Gentry et al., 2006) and 160 m between the BS and VFW locations results in arrival times of 67–72 days with no longitudinal dispersion. The actual arrival time was at least 155 days, suggesting some vertical impedance during infiltration or lower hydraulic conductivity. The results were further complicated by pumping from the pool well in April 2015, which may have hastened the migration of the Br^- plume past the screened interval of the VFW. Although the Br^- tracer results do not provide recharge rate information, they do confirm that a vertical recharge pathway exists from the sandy soils along the hillslopes to the water table of the Memphis aquifer.

Alkalinity and nitrate concentrations at the BS location were consistently elevated above those observed at other locations, providing an additional tracer for vertical infiltration at the BS location. A septic system and leach field are located underneath the hillslope, at less than a meter depth, approximately 30 m uphill from the BS location. Runoff from septic leach fields characteristically has high nitrate and alkalinity concentrations (Seiler, 1999), resulting in elevated nitrate and alkalinity in soils located down gradient of the leach field along the hillslope. A binary mixing model was applied to assess the percent of nitrate-rich water infiltrated at the BS location that reaches the water table. VFW is down-gradient from the BS location, and consistently has the lowest observed level for the water table in the study area. The DPW and Pool well are used as potential end-member water compositions, representing “normal” groundwater nitrate levels. SS2 is not viable, as its nitrate concentration is greater than that of VFW, suggesting some of the infiltrating leachate waters percolated to the SS2 well. The results of the mixing model indicate 1–9 % of total recharge is occurring by vertical infiltration at the BS location, likely following the pathway identified with the Br^- tracer and reaching the VFW. The remaining percentage (91–99 %) of recharge must come from another source, either lateral flow, other hillslopes adjacent to VFW, or unknown sources.

4.3. Lateral recharge

Groundwater elevtion, water chemistry and environmental tracer data provide evidence for significant lateral recharge to the Memphis aquifer at the Pinecrest site. The upland monitoring wells (SS2 and VFW) show rise and fall in groundwater elevation opposite those of seasonal wetness and dryness, suggesting lag in response or additional water sources. In contrast, the groundwater elevation in the DPW was highly influenced by seasonal precipitation and stream flow, with higher sustained water levels during wetter times of the year. For the majority of the year, DPW maintained the highest groundwater elevation of the three wells. During the dryer months, it dropped to levels similar to those observed in SS2. However, water levels never dropped below those observed in the VFW. These observations indicate a persistent lateral gradient from DPW to VFW and from DPW toward the Wolf River where surface flow discharges from the watershed (Fig. 11).

Lateral groundwater flow under unconfined conditions was calculated using Darcy’s law and the range of hydraulic conductivity of 3.7–4.0 m/d. Groundwater levels were averaged during the months that water levels at DPW were substantially higher than VFW (March – August 2014, and December 2014 – February 2015). Average specific discharge for these periods was 1.4–1.5 m/d for DPW to VFW and 0.66 to 0.72 m/d for SS2 to VFW. The estimated travel time for water to move from DPW to VFW is 110–119 days, and from SS2 to VFW is 112–121 days. These travel time estimates are consistent with a rise in VFW groundwater level approximately 3–4 months after peak groundwater level in DPW. However, the data do not explain why SS2 shows similar trend to VFW. Sources outside the monitored area could be contributing lateral recharge to SS2, such as another surface water source or adjacent watershed.

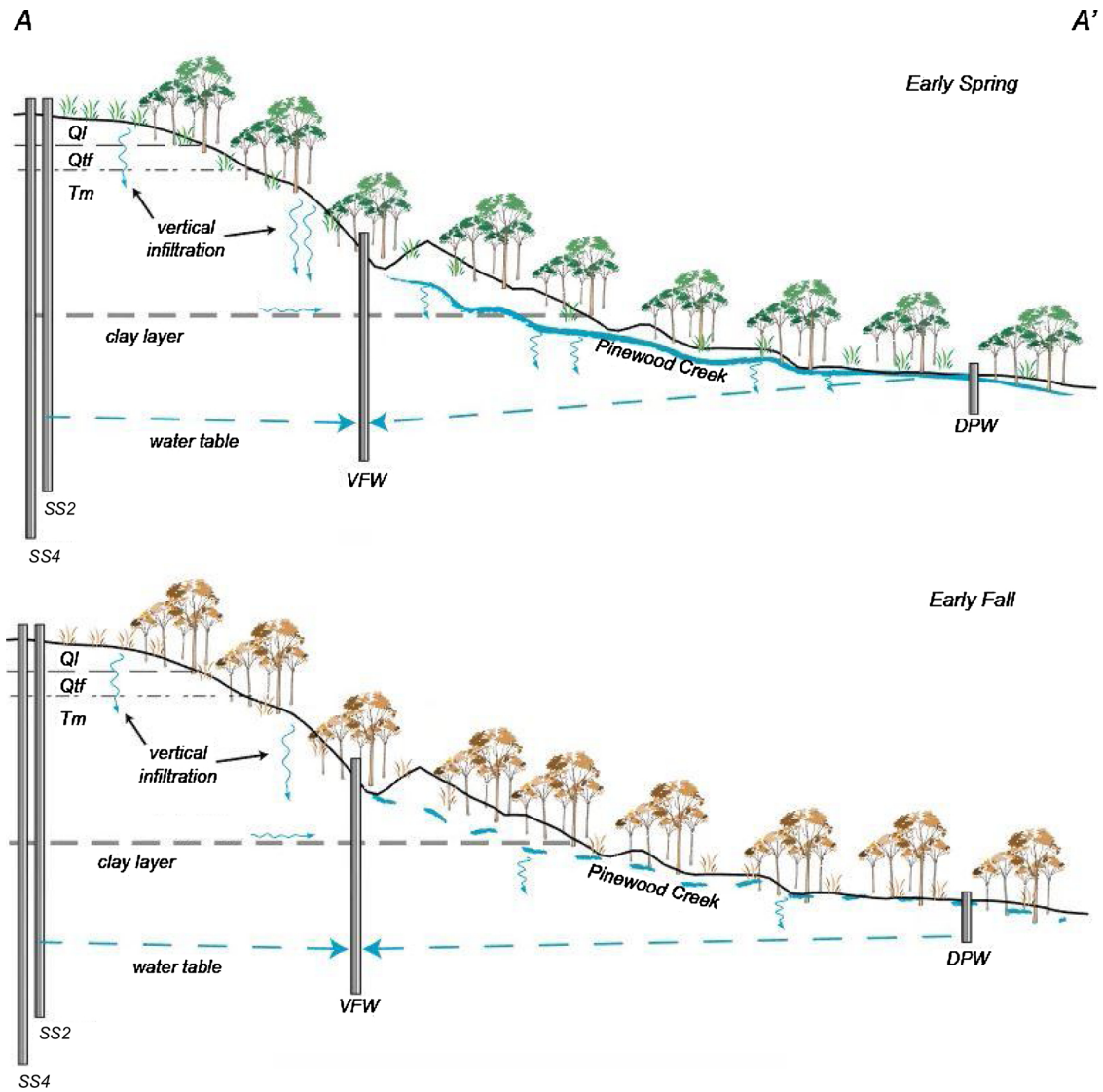

Fig. 11. Conceptual model of groundwater flow at the Pinecrest site. A-A' corresponds to Fig. 1. Depths and water levels are not to scale. Ql – Quaternary loess, Qtf – Quaternary fluvial terrace deposits, Tm – Tertiary (Eocene) Memphis Sand. (request color image).

The time frame and monitored area of the present study are insufficient to assess the recharge source for the SS2 well.

The chemistry of the groundwater is distinctly different than that of precipitation and soil water, but similar to that of surface water. Precipitation is dilute and acidic, as is typical for the southeastern part of North America (Lajtha and Jones, 2013), with mixed cation HCO_3-SO_4 composition. In contrast, soil water from the lysimeters is pH-neutral, moderate specific conductance 100 to 1400 µS, and Na-HCO_3-SO_4 composition. The seasonal shift in soil water composition is likely related to an increased proportion of sulfate in winter and spring precipitation followed by a proportional increase in bicarbonate during evaporation and soil water-deficit during summer and fall. The groundwater is slightly acidic, low specific conductance (30–140 µS), and mixed cation-HCO_3 composition. Although groundwater was sampled only once during the year, substantial changes in groundwater chemistry are unlikely over the period of a year absent strong gradients in groundwater chemistry or hydraulic head. Surface water chemistry had similar pH and specific conductance to groundwater, but ranged from mixed cation-HCO_3 to mixed cation-HCO_3-SO_4 composition.

The strong similarity of surface water composition to groundwater suggests that infiltrated stream water is a significant component of the groundwater, whereas infiltrated soil water from the upland soils does not contribute substantially to groundwater. Surface water is mainly immediate runoff from precipitation events that has not interacted extensively with soil minerals. Surface water from late winter or early spring may have more interaction with soils as indicated by the sulfate-rich composition of PWC water from 3/28/14, likely due to protracted soil-water saturation and runoff. Chemical reaction of acidic, dilute precipitation with soil minerals should result in pH-neutral water of mixed composition rather than the observed Na-SO_4 composition of soil water, suggesting reaction with a sodium- and sulfate-bearing soil phase. The most likely source for concentration of these elements in the soil is

deposition of aerosols and particulates from atmospheric plumes emanating from a coal-fired power plant and oil refinery in Memphis (75 km west of Pinecrest) that have been operational since the 1940s and 1950s. Sulfate, either as adsorbed SO_2 on particulate matter or in mineral form in fine ash, is a well-established reactive by-product of coal combustion (Smith and Gruber, 1966; Kang et al., 2011) and atmospheric concentrations are correlated with fossil fuel energy use (Lajtha and Jones, 2013). Sodium is preferentially released relative to other alkaline earth and alkaline metals during the combustion of coal (Li et al., 2015) and may also be a significant mineral component of ash (Smith and Gruber, 1966). Given the oxidizing conditions in groundwater, sulfate reduction is not viable as a removal process. Furthermore, a mechanism does not exist to exchange the sodium in the soil water for the mixed cation composition observed in groundwater. Thus, the soil water is unlikely to be a significant source of recharge water for groundwater. This conclusion is also consistent with the slow vertical recharge rates through the upland soils based on the vadose-zone chloride profile and nitrate mixing model calculations.

Modeling of the SF_6 and ^3H tracer concentrations suggests lateral groundwater flow of modern water by piston-flow rather than percolation through a thick vadose zone. Fig. 10 shows that the data for VFW and SS2 fit a PFM, which is consistent with short recharge pathways and minimal dispersion. Vertical infiltration through the thick vadose zone would result in substantial hydrodynamic dispersion during percolation and lack of coherent behavior of SF_6, a gas, and ^3H, a component of the water molecule, during equilibration with soil gases (Solomon and Cook, 1995). Studies of infiltrated environmental tracers through thick vadose zones commonly show binary mixing relationships with shallow groundwater of other sources (Santoni et al., 2016). Consistent with observed water chemistry and hydrologic calculations above, the yearly recharge of surface water to groundwater in exposed Memphis Sand near DPW drives lateral groundwater flow, which allows ^3H and SF_6 to migrate seasonally with minimal lateral mixing consistent with piston-flow behavior.

4.4. Significance for recharge processes

The results of the present study indicate a strong lithological control on recharge rates and pathways to the underlying unconfined Memphis aquifer. Vadose and saturated zone CMB and water-balance estimates for recharge rates through the upland surfaces and alluvial valleys at Pinecrest are less than 16 mm/yr. Yearly variation in groundwater elevation at VFW and SS2 are 100–200 mm/yr, which, assuming a 30 % porosity of the Memphis Sand, requires a recharge of at least 70–140 mm/yr. Water chemistry and tracer data provide strong evidence that the main source of recharge is infiltrated surface water. Given that precipitation, vegetation, and land-use in the areas of exposed Memphis Sand and the upland areas are not grossly different, the main difference in the recharge rate is argued to be due to lithology and the presence of preferential recharge pathways through transmissive sediments. The loess, fluvial terrace deposits and upper 2–3 m Memphis Sand each have varying degrees of soil development, mainly in the form of accumulated clays in the B horizons (Larsen and Brock, 2014). Accumulated clay and soil formation are minimal in the exposed Memphis Sand and sandy surface soils formed therein. Given that loess and underlying paleosols mantle most landscape surfaces throughout western Tennessee and other states in the Mississippi embayment, recharge is likely to be focused where fluvial incision has removed the loess and paleosols exposing underlying sandy formations, primarily along modern alluvial valleys.

Similar lithological control on recharge is observed in other regions mantled by loess or other fine-grained deposits. Studies of recharge through loess in northern China show similar behavior to that of the western Tennessee area but differences as well. Several studies have noted anomalously high tritium or agricultural chemicals and low chloride in groundwater underlying loess regions and have argued for focused recharge in deep gullies or alluvial valleys (Lin and Wei, 2006; Gates et al., 2011). However, other studies have shown groundwater underlying loess regions being dominated by pre-modern water with slow infiltration through the loess being the dominant recharge mechanism (e.g., Huang et al., 2017). A critical aspect of rapid recharge in thick loess regions, such as that in China, may be the availability of focused recharge pathways in topographic depressions and deep gullies (Gates et al., 2011). Similar observations have been made in regions mantled by glacial till, where recharge is focused in the alluvial valleys incised through the till (Gates et al., 2014). Studies is Coastal Plain deposits of western Australia show similar sensitivity to the permeability of surface soils (Johnston, 1987a; b; Dawes et al., 2012).

Recharge rates in western Tennessee vary in relation to the proportion of loess and fine-grained surface soils suggesting that recharge has greater sensitivity to land use and climate changes. Early research in the Memphis aquifer of western Tennessee considered diffuse percolation through the loess to be the dominant source of recharge (Parks and Carmichael, 1990). Modeling of groundwater flow in the Memphis area by Brahana and Broshears (2001) showed that 42 % of the hydrologic budget of the Memphis aquifer is recharge in the outcrop belt, with almost all other water coming from vertical leakage through a shallow aquifer primarily in alluvial valleys. Numerically derived recharge rates in modeling studies within the region range from 3 to 36 mm/yr (Arthur and Taylor, 1998; Brahana and Broshears, 2001; McKee and Clark, 2003); however, these values are determined by model fit and not measured. The present study shows that less than 16 mm/yr of recharge is likely in loess-covered regions, which is less than that typically observed in eastern North America (median of 43–59 mm/yr using similar methods, Nolan et al., 2007). Studies in western Tennessee where incision has largely removed loess and paleosol-bearing deposits from alluvial valleys yield recharge rates based on water balance of about 300–900 mm/yr (Simco, 2018; Smith, 2019), with only minor recharge attributed to the loess-mantled upland surfaces. Similarly, recharge rates based on Q_{60} and Q_{65} (percent duration flow) relationships to estimate mean annual base flow in areas within the region with sand aquifers and little or no loess cover range from 127 to 229 mm/yr (Stricker, 1983; Bailey, 1993). Geologic mapping of two quadrangles in the Memphis Sand outcrop belt indicated that less than 7 % of the mapped area is underlain by sandy soils, with about 20 % of the mapped area as alluvium (Brock, 2012). These results indicate that recharge to the Memphis aquifer is highly focused in as little as 7 % of the outcrop belt, although leakage contributions through sandy alluvium may occur over a somewhat greater area. Land-use changes can both increase and decrease potential for recharge, depending on the type of surface

modification that is made. Future development in the loess-covered regions of western Tennessee needs to closely consider how land surface changes may affect recharge to the regional aquifers to ensure sustainability of groundwater resources.

5. Conclusions

The results of this study indicate that recharge is largely controlled by lithology of surface soils and outcrop of the underlying Memphis Sand, with recharge focused along modern alluvial valleys and other areas where the Memphis Sand is exposed. Using the vadose-zone and saturated zone CMB methods and water balance yields annual recharge rates from 4.2–16 mm/yr, indicating that recharge through loess and underlying paleosols on upland surfaces is not sufficient to account for the observed annual water-table fluctuations of 100–200 mm/yr. Rather, hydrochemistry, environmental tracer concentrations and groundwater flow indicate that recharge is dominated by stream seepage in sandy stream beds on subcropping Memphis Sand and lateral recharge beneath upland surfaces. With as little as 7 % exposure of the Memphis Sand in the unconfined region of the aquifer and another 13 % of the area as alluvial valleys, recharge to the Memphis aquifer is limited to preferential paths of recharge in the landscape. As such, the sustainability of the aquifer, which is currently providing as much as 210 million gallons per day (Maupin et al., 2014) for Memphis, Tennessee, and surrounding areas, may be highly sensitive to alteration of land use that affects the access to preferential pathways of recharge. Evidence for groundwater recharge through preferential pathways is known from other regions with loess or other fine-grained soils at the land surface, indicating this phenomenon may be of broader importance than currently appreciated in regard to the groundwater resources.

Acknowledgements

This research was funded through the University of Memphis Ground Water Institute, and U.S. Geological Survey Water Resources Research Center grants to Larsen and Waldron. Field site access was granted by the Presbytery of the Mid-South Pinecrest Camp. Christopher Garner and Jason Morat assisted with chloride extraction and analysis from the vadose-zone borehole. Mary Dubose, Haley Gallo, and Sarah Girdner assisted with field work during the 2013-2015 research at Pinecrest Camp. A previous version of the manuscript was improved by review comments from an anonymous reviewer.

Appendix A. Geochemical Data

Table A1
Soil water sample field data.

Sample Name	Sample Date	Field Temp. (°C)	Field pH	Field S.C. (µS)	Field D.O. (mg/L)	Lab Alk. (mg/L)
SSL1 3/14	3/14/2014	12.3	6.10	465	9.30	111
SSL2 3/14	3/14/2014	12.3	5.60	136	9.80	33.9
SSL3 3/14	3/14/2014	13.3	5.10	51.8	8.20	12.9
GFL1 3/14	3/14/2014	17.3	7.20	403	9.90	168
GFL2 3/14	3/14/2014	19.3	6.61	716	9.80	39.3
GFL3 3/14	3/14/2014	17.0	5.17	108	8.80	14.2
BSL1 3/14	3/14/2014	22.7	7.98	677	9.40	nd
BSL2 3/14	3/14/2014	18.6	7.00	96.0	8.70	64.2
BSL3 3/14	3/14/2014	20.1	7.20	1418	8.50	112
VFL2 3/14	3/14/2014	16.4	7.20	835	7.40	281
VFL3 3/14	3/14/2014	14.9	5.50	291	10.3	13.9
SSL1 4/11	4/11/2014	21.3	6.72	360	8.50	75.2
SSL2 4/11	4/11/2014	19.1	5.99	121	8.00	34.6
SSL3 4/11	4/11/2014	20.3	5.59	54.0	3.80	13.7
GFL1 4/11	4/11/2014	24.1	7.34	364	8.50	161
GFL2 4/11	4/11/2014	23.4	6.68	543	8.10	42.7
GFL3 4/11	4/11/2014	22.9	5.56	117	5.50	19.8
BSL2 4/11	4/11/2014	27.2	7.19	815	6.25	80.8
BSL3 4/11	4/11/2014	25.0	7.66	702	8.00	125
VFL1 4/11	4/11/2014	24.2	7.80	422	8.00	293
VFL2 4/11	4/11/2014	21.7	7.86	651	5.39	248
VFL3 4/11	4/11/2014	20.0	5.57	256	5.80	12.9
SSL1 5/23	5/23/2014	21.1	6.66	208	7.30	134
SSL2 5/23	5/23/2014	23.4	6.40	214	5.10	93.2
SSL3 5/23	5/23/2014	23.9	5.79	97.9	4.80	34.6
GFL1 5/23	5/23/2014	26.2	7.40	206	6.60	209
GFL2 5/23	5/23/2014	23.9	6.58	413	7.10	64.7
GFL3 5/23	5/23/2014	22.6	6.22	184	5.80	47.1
BSL2 5/23	5/23/2014	24.5	7.21	624	7.10	131
BSL3 5/23	5/23/2014	25.5	7.57	1166	7.40	152
VFL1 5/23	5/23/2014	26.8	7.57	618	7.10	363

(*continued on next page*)

Table A1 (*continued*)

Sample Name	Sample Date	Field Temp. (°C)	Field pH	Field S.C. (μS)	Field D.O. (mg/L)	Lab Alk. (mg/L)
VFL2 5/23	5/23/2014	23.9	7.36	680	7.30	333
VFL3 5/23	5/23/2014	22.1	5.86	221	6.50	26.4
SSL1 7/18	7/18/2014	25.0	7.08	330	nd	97.8
SSL2 7/18	7/18/2014	19.1	6.40	148	nd	59.5
SSL3 7/18	7/18/2014	19.0	5.50	68.1	nd	26.4
GFL1 7/18	7/18/2014	19.3	7.30	494	nd	286
GFL2 7/18	7/18/2014	19.6	6.57	246	nd	63.0
GFL3 7/18	7/18/2014	19.5	6.31	156	nd	47.8
BSL2 7/18	7/18/2014	19.6	7.37	521	nd	175
BSL3 7/18	7/18/2014	19.5	7.55	897	3.50	222
VFL1 7/18	7/18/2014	19.1	7.23	690	nd	389
VFL3 7/18	7/18/2014	19.1	6.56	91.3	nd	34.4
SSL1 9/17	9/17/2014	25.0	7.10	291	7.70	113
SSL2 9/17	9/17/2014	9.00	6.73	131	nd	34.6
SSL3 9/17	9/17/2014	25.9	6.02	141	6.80	41.2
GFL3 9/17	9/17/2014	25.7	7.08	69.4	7.50	37.6
BSL2 9/17	9/17/2014	23.5	7.59	194	8.70	108
BSL3 9/17	9/17/2014	23.0	7.68	87.9	7.00	217
VFL1 9/17	9/17/2014	22.8	7.56	565	7.10	298
VFL2 9/17	9/17/2014	23.1	7.73	415	7.70	447
VFL3 9/17	9/17/2014	23.1	6.82	76.8	8.10	24.2
SSL1 10/15	10/15/2014	19.8	7.06	290	8.70	121
SSL2 10/15	10/15/2014	19.8	6.64	155	7.15	54.7
SSL3 10/15	10/15/2014	20.0	6.21	135	6.55	38.6
BSL2 10/15	10/15/2014	18.7	7.92	243	8.60	nd
BSL3 10/15	10/15/2014	17.9	8.05	454	8.95	166
VFL1 10/15	10/15/2014	19.1	7.42	514	7.85	299
VFL2 10/15	10/15/2014	18.8	7.62	393	8.40	303
SSL1 11/12	11/12/2014	10.1	6.74	324	9.40	81.7
SSL2 11/12	11/12/2014	9.90	6.89	280	8.80	117
SSL3 11/12	11/12/2014	9.70	6.04	62.5	7.25	15.9
BSL2 11/12	11/12/2014	9.80	7.84	357	7.20	117
VFL1 11/12	11/12/2014	8.00	7.71	630	11.3	326
VFL2 11/12	11/12/2014	9.40	7.45	782	7.60	396
SSL1 12/9	12/9/2014	10.6	6.56	301	8.80	67.8
SSL3 12/9	12/9/2014	11.5	5.81	56.7	6.80	13.4
GFL3 12/9	12/9/2014	10.5	6.55	86.9	7.80	12.4
VFL1 12/9	12/9/2014	10.8	7.57	622	9.10	303
VFL2 12/9	12/9/2014	11.2	7.34	709	7.80	368
VFL3 12/9	12/9/2014	10.9	6.46	126	7.40	13.4
SSL1 1/5	1/5/2015	5.40	6.56	305	10.2	73.7
SSL2 1/5	1/5/2015	6.50	6.60	201	8.50	78.3
SSL3 1/5	1/5/2015	7.50	5.82	55.0	6.80	13.7
GFL1 1/5	1/5/2015	7.70	7.37	232	7.00	192
GFL2 1/5	1/5/2015	8.80	6.55	237	9.20	36.4
GFL3 1/5	1/5/2015	9.00	6.80	128	7.40	24.2
BSL1 1/5	1/5/2015	6.80	7.74	877	9.00	nd
BSL2 1/5	1/5/2015	6.80	7.85	466	8.80	171
BSL3 1/5	1/5/2015	6.90	7.95	915	7.40	nd
VFL1 1/5	1/5/2015	8.50	7.08	517	8.80	281
VFL2 1/5	1/5/2015	8.50	6.89	305	7.80	310
VFL3 1/5	1/5/2015	8.4	6.18	200	7.40	35.4
SSL1 2/4	2/4/2015	9.80	6.56	287	7.00	66.6
SSL2 2/4	2/4/2015	9.70	6.56	119	9.00	61.0
SSL3 2/4	2/4/2015	10.5	5.88	59.9	5.50	13.9
GFL3 2/4	2/4/2015	13.4	6.28	85.7	6.52	16.3
BSL2 2/4	2/4/2015	14.8	7.50	265	7.90	nd
BSL3 2/4	2/4/2015	13.8	7.78	712	8.40	273
VFL2 2/4	2/4/2015	11.6	7.21	569	7.50	280
VFL3 2/4	2/4/2015	12.6	6.42	173	7.50	37.3

L1, L2, and L3 represent lysimeters at depths of 0.5, 1.0, and 1.5 m.
nd - no data.

Table A2
Water chemistry data.

Sample Name	F^- (mg/l)	Cl^- (mg/l)	NO_2^- (mg/l)	Br^- (mg/l)	NO_3^- (mg/l)	PO_4^{3-} (mg/l)	SO_4^{2-} (mg/l)	Na^+ (mg/l)	Ca^{2+} (mg/l)	K^+ (mg/l)	Mg^{2+} (mg/l)	Mn^{2+} (mg/l)	Fe^{2+} (mg/l)
Rain 3/14	0.379	0.101	bd	bd	0.443	0.187	0.864	0.236	0.0850	bd	0.0203	bd	0.0180
SSL1 3/14	0.0716	0.983	bd	bd	0.264	bd	120	86.8	2.66	0.936	1.96	bd	bd
SSL2 3/14	0.0301	0.730	bd	bd	0.118	bd	30.9	24.4	0.165	0.0704	0.299	bd	bd
SSL3 3/14	0.0173	0.972	bd	bd	0.312	bd	9.75	8.72	0.766	0.324	0.653	bd	bd
GFL1 3/14	0.342	1.10	bd	bd	0.0986	0.716	51.3	82.7	0.760	1.37	0.0740	bd	bd
GFL2 3/14	0.0382	1.12	bd	bd	10.6	bd	251	126	1.78	0.870	1.95	bd	bd
GFL3 3/14	0.0248	1.62	bd	bd	0.375	bd	30.5	15.9	0.622	0.650	1.05	0.0367	bd
BSL2 3/14	0.103	1.97	bd	bd	7.50	bd	333	188	2.01	2.37	0.604	bd	0.525
BSL3 3/14	0.145	2.18	bd	bd	50.6	bd	507	276	4.38	3.54	1.98	bd	bd
VFL2 3/14	0.144	0.406	bd	bd	0.242	bd	170	176	0.160	2.62	bd	bd	bd
VFL3 3/14	0.0101	0.932	bd	bd	bd	bd	101	47.7	1.53	0.444	1.18	bd	bd
PWC 3/28	0.0293	12.4	0.104	bd	0.132	bd	*9.82*	6.49	4.43	1.88	1.46	0.184	1.56
Rain 4/11	0.0103	2.80	0.172	bd	0.476	3.61	30.5	0.482	0.322	2.67	0.332	bd	bd
SSL1 4/11	0.101	1.08	bd	bd	0.540	bd	24.8	60.5	0.650	0.187	1.31	bd	bd
SSL2 4/11	0.0440	0.427	bd	bd	0.168	bd	10.9	23.2	0.0830	0.0743	0.146	bd	bd
SSL3 4/11	0.0124	0.904	0.0179	bd	0.0675	bd	39.8	7.56	0.293	0.165	0.578	bd	bd
GFL1 4/11	0.380	0.906	bd	bd	0.145	0.656	*197*	80.9	0.380	1.50	bd	0.536	bd
GFL2 4/11	0.117	0.904	bd	bd	14.6	bd	31.3	109	1.11	1.08	1.07	bd	bd
GFL3 4/11	bd	1.26	bd	bd	0.832	bd	*284*	18.8	0.494	0.559	0.769	bd	bd
BSL2 4/11	0.113	1.09	bd	bd	10.1	bd	*534*	165	2.02	2.16	0.360	bd	bd
BSL3 4/11	bd	0.634	2.95	bd	bd	bd	23.8	279	5.64	4.79	1.80	bd	bd
VFL1 4/11	0.319	0.275	bd	bd	0.0195	bd	109	96.9	0.100	1.60	bd	bd	bd
VFL2 4/11	0.176	0.330	bd	bd	0.205	bd	88.5	139	0.680	1.02	bd	bd	bd
VFL3 4/11	0.0299	0.734	bd	bd	0.0235	bd	7.82	43.2	1.22	0.432	0.769	bd	bd
Rain 5/23	0.0183	0.526	bd	bd	0.496	bd	0.886	0.254	0.558	0.119	0.0636	bd	bd
SSL1 5/23	0.0986	0.850	bd	bd	0.142	bd	88.1	97.5	1.80	0.904	1.46	bd	bd
SSL2 5/23	0.0568	0.153	bd	bd	0.109	bd	23.6	42.0	0.340	2.82	0.131	0.571	bd
SSL3 5/23	0.0262	0.896	bd	bd	0.221	bd	20.5	17.1	0.461	0.259	0.554	0.0181	bd
GFL1 5/23	0.659	0.653	bd	bd	0.0915	0.181	34.9	101	1.66	2.70	0.315	bd	bd
GFL2 5/23	0.0501	0.674	bd	bd	6.43	bd	120	90.3	0.560	1.26	0.510	bd	bd
GFL3 5/23	0.0422	1.04	bd	bd	2.54	bd	40.8	33.6	0.251	0.679	0.391	bd	bd
BSL2 5/23	0.144	0.782	bd	bd	15.2	bd	154	133	2.78	2.29	bd	bd	bd
BSL3 5/23	0.178	1.48	bd	bd	50.5	bd	364	217	4.56	4.36	1.13	5.07	bd
VFL1 5/23	0.294	0.189	bd	bd	bd	bd	18.3	168	0.960	3.56	0.944	1.34	bd
VFL2 5/23	0.152	0.171	bd	bd	0.0213	bd	60.4	173	0.560	2.04	bd	bd	bd
VFL3 5/23	0.0134	0.507	bd	bd	bd	bd	67.4	32.3	1.47	1.06	0.798	bd	bd
Rain 7/18	bd	0.162	bd	bd	bd	bd	0.947	0.146	0.475	0.064	0.114	bd	0.165
SSL1 7/18	0.0965	0.201	bd	bd	bd	bd	69.7	68.0	0.960	0.799	0.907	2.29	bd
SSL2 7/18	bd	0.180	bd	bd	0.0948	bd	21.1	35.8	0.139	0.269	0.166	bd	bd
SSL3 7/18	0.0330	0.886	bd	bd	0.274	bd	10.8	11.3	0.365	0.241	0.278	bd	bd
GFL1 7/18	0.283	0.360	bd	bd	0.204	0.263	27.9	112	0.290	2.37	1.18	3.87	bd
GFL2 7/18	0.0397	0.444	bd	bd	bd	bd	60.9	45.1	bd	1.30	0.467	bd	bd
GFL3 7/18	0.0458	1.00	bd	bd	1.49	bd	28.9	29.1	0.291	0.828	0.300	0.153	bd
BSL3 7/18	0.218	0.819	bd	bd	31.6	bd	161	214	2.88	3.64	0.436	4.19	bd
VFL1 7/18	0.217	0.146	bd	bd	0.736	bd	13.9	155	0.760	4.62	bd	0.103	bd
VFL3 7/18	0.0324	0.384	bd	bd	bd	bd	52.6	22.8	1.07	0.636	0.738	0.461	bd
VFW 8/4	0.0355	6.75	bd	0.0160	2.83	bd	1.08	8.48	5.08	0.821	1.48	0.314	1.51
Pool Well 8/4	bd	1.49	bd	0.0105	2.49	bd	0.133	2.11	1.45	0.479	0.433	bd	0.0350
Pool Water 8/4	bd	17.7	bd	bd	3.06	bd	0.314	27.5	11.43	0.133	0.345	bd	bd
E. Creek 8/6	0.0262	1.11	bd	bd	0.23	0.024	3.13	1.33	5.12	0.966	1.03	0.0275	0.114
PWC Joint 8/6	0.0307	1.36	0.0141	bd	0.46	bd	2.71	1.53	5.90	0.983	1.14	0.171	0.231
DPW 8/6	bd	1.13	0.0176	bd	0.0654	bd	4.09	1.41	1.34	0.592	0.854	bd	0.783
SS2 8/6	bd	1.94	bd	bd	3.21	0.014	0.163	2.40	1.89	1.31	0.664	bd	0.106
Rain 9/17	0.422	0.384	bd	bd	0.757	bd	0.678	0.193	0.373	0.0629	0.0630	bd	0.281
SSL2 9/17	0.0954	0.657	bd	bd	0.0741	bd	26.5	19.5	0.215	0.212	0.0809	4.88	bd
SSL3 9/17	0.0555	1.08	bd	bd	0.457	bd	25.8	14.2	0.347	0.310	0.291	0.260	bd
GFL3 9/17	0.0372	1.25	bd	bd	5.40	bd	24.9	45.0	0.659	0.851	0.501	0.467	0.232
BSL3 9/17	0.337	0.705	bd	bd	*28.3*	bd	*188*	106	3.51	2.59	0.990	bd	0.110
VFL1 9/17	0.210	0.242	bd	bd	0.745	bd	20.0	75.0	3.98	2.19	0.0990	bd	bd
VFL2 9/17	0.174	0.093	bd	bd	0.787	bd	52.4	161	2.16	2.55	0.223	bd	bd
VFL3 9/17	0.0121	0.340	bd	bd	0.0908	bd	*43.7*	19.0	1.36	0.690	0.0828	bd	bd
Rain 10/15	bd	0.318	0.0105	bd	0.153	0.574	0.769	0.237	0.288	0.501	0.0586	bd	bd
SSL1 10/15	0.253	0.996	bd	bd	0.0525	bd	48.0	67.7	2.56	0.756	0.713	bd	bd
SSL2 10/15	0.0954	0.390	bd	bd	0.0192	bd	24.9	43.5	0.156	0.201	0.0515	bd	bd
SSL3 10/15	0.0538	1.26	bd	bd	0.248	bd	24.0	15.6	0.238	0.290	0.222	bd	bd
BSL3 10/15	0.346	1.01	bd	bd	22.7	bd	198	119	3.85	2.80	1.14	bd	bd
VFL1 10/15	0.201	0.315	bd	bd	0.564	bd	21.7	109	0.740	3.26	0.0110	bd	bd

(*continued on next page*)

Table A2 (*continued*)

Sample Name	F^- (mg/l)	Cl^- (mg/l)	NO_2^- (mg/l)	Br^- (mg/l)	NO_3^- (mg/l)	PO_4^{3-} (mg/l)	SO_4^{2-} (mg/l)	Na^+ (mg/l)	Ca^{2+} (mg/l)	K^+ (mg/l)	Mg^{2+} (mg/l)	Mn^{2+} (mg/l)	Fe^{2+} (mg/l)
VFL2 10/15	0.219	0.25	bd	bd	1.09	bd	56.2	115	2.05	2.47	3.58	bd	bd
Rain 11/12	0.038	0.346	0.0114	bd	0.595	bd	0.680	0.393	0.439	0.0575	0.0264	bd	bd
SSL1 11/12	0.128	0.917	bd	bd	0.0760	bd	66.6	60.5	1.45	0.652	0.914	bd	bd
SSL2 11/12	0.117	0.774	bd	bd	0.0399	bd	24.0	55.3	0.500	1.18	0.753	bd	3.30
SSL3 11/12	0.0371	1.09	bd	bd	0.194	bd	8.71	9.53	0.205	0.210	0.258	bd	bd
BSL2 11/12	0.181	0.829	bd	bd	8.64	0.503	62.7	80.5	2.29	1.50	0.119	bd	bd
VFL1 11/12	0.162	0.393	bd	bd	0.674	bd	24.4	137	0.680	2.68	bd	bd	bd
VFL2 11/12	0.126	0.114	bd	bd	0.610	bd	50.1	176	1.48	3.56	0.292	1.80	bd
Rain 12/9	bd	0.417	bd	bd	0.424	bd	0.481	0.236	0.120	0.0595	bd	0.0808	bd
SSL1 12/9	0.0525	0.715	bd	bd	0.0301	bd	73.8	54.5	0.820	1.24	1.01	bd	bd
SSL3 12/9	0.0178	1.21	bd	bd	0.123	bd	9.98	9.26	0.273	0.219	0.416	0.145	bd
GFL3 12/9	0.0310	1.10	bd	bd	0.0376	bd	20.9	11.4	0.146	0.582	0.267	bd	2.01
VFL1 12/9	0.151	0.554	bd	bd	bd	bd	20.9	148	0.940	2.48	bd	bd	bd
VFL2 12/9	0.105	0.159	bd	bd	0.609	bd	46.3	151	0.800	2.45	0.0420	bd	bd
VFL3 12/9	0.0114	0.389	bd	bd	bd	bd	38.7	10.5	1.10	0.637	0.797	bd	bd
Rain 1/5	0.0408	0.144	bd	bd	0.805	bd	0.762	0.168	0.195	0.0347	0.0143	0.0116	bd
SSL1 1/5	0.0598	0.701	bd	bd	0.0327	bd	64.8	54.9	1.28	0.559	1.39	bd	bd
SSL2 1/5	0.0673	0.287	bd	bd	0.0619	bd	25.5	36.1	0.320	0.251	0.184	bd	bd
SSL3 1/5	0.0207	1.12	bd	bd	0.124	bd	9.56	8.22	0.279	0.231	0.414	0.0707	bd
GFL1 1/5	0.214	1.19	bd	bd	0.0332	bd	51.5	95.1	0.560	1.54	0.165	bd	bd
GFL2 1/5	0.0426	1.01	bd	bd	0.0515	bd	60.8	38.8	0.280	0.945	0.537	0.386	bd
GFL3 1/5	0.0320	1.05	bd	bd	0.0346	bd	28.5	18.4	0.258	0.861	0.401	0.255	0.0830
BSL2 1/5	0.249	1.34	bd	bd	3.38	1.19	74.9	91.0	2.94	1.19	0.225	1.99	1.13
VFL1 1/5	0.143	0.681	bd	bd	0.0158	bd	15.0	111	0.680	1.89	0.0830	0.797	bd
VFL2 1/5	0.124	0.251	bd	bd	bd	bd	37.7	118	0.620	1.48	0.452	0.128	bd
VFL3 1/5	0.0282	0.395	bd	bd	0.0693	bd	51.6	29.3	0.920	0.554	0.512	bd	bd
Rain 2/4	0.875	0.239	bd	bd	1.06	bd	0.783	0.196	0.381	0.0266	0.0318	0.154	bd
SSL1 2/4	0.0497	0.609	bd	bd	bd	bd	65.4	51.1	0.900	0.268	1.23	0.733	bd
SSL2 2/4	0.0383	0.163	bd	bd	bd	bd	21.9	8.34	0.227	0.204	0.400	0.0939	bd
SSL3 2/4	0.0185	1.02	bd	bd	0.0463	bd	10.7	33.9	0.108	0.124	0.161	bd	bd
GFL3 2/4	0.0201	1.11	bd	bd	0.126	bd	21.2	13.8	0.258	0.792	0.577	0.220	bd
BSL3 2/4	0.329	0.713	bd	bd	7.97	bd	103	139	2.41	1.80	0.647	bd	bd
VFL2 2/4	0.0908	0.142	bd	bd	bd	bd	36.0	132	1.10	1.70	0.0960	0.669	bd
VFL3 2/4	bd	0.307	bd	bd	bd	bd	48.9	34.2	bd	0.340	0.0460	8.02	bd
Rain 2/25	0.0224	8.64	0.162	bd	0.0273	bd	4.20	0.337	0.218	0.0472	0.0332	0.178	bd
PWC 2/25	bd	0.618	bd	bd	0.725	bd	0.827	4.15	2.00	3.70	0.862	0.104	bd

bd = below detection.
L1, L2, and L3 represent lysimeters at depths of 0.5, 1.0, and 1.5 m.
Values in italics indicate concentrations above calibration range, with no diluted samples available.

Appendix B. Hydraulic conductivity from soil and sediment samples in neutron probe boreholes (NP), lysimeter boreholes (L1), and well borehole (BH) samples and slug tests

Location, type, depth	Elevation of sample or screen mid-point (m)	Mean Grain size (mm)	Hydrologic unit	Shepherd (m/day)
BS NP (0.00–0.25) m	155.75	0.315	Sandy soil	5.39
BS NP (0.25–0.50) m	155.50	0.358	Sandy soil	6.53
BS NP (0.50–0.75) m	155.25	0.406	Sandy soil	7.89
BS NP (0.75–1.00) m	155.00	0.403	Sandy soil	7.80
BS NP (1.00–1.25) m	154.75	0.247	Sandy soil	3.74
BS NP (1.25–1.50) m	154.50	0.376	Sandy soil	7.03
BS NP (1.50–1.75) m	154.25	0.140	Memphis paleosol	1.60
BS NP (1.75–2.00) m	154.00	0.141	Memphis paleosol	1.61
BS NP (2.00–2.25) m	153.75	0.154	Memphis paleosol	1.84
BS NP (2.25–2.50) m	153.50	0.257	Memphis paleosol	3.97
BS NP (2.50–2.75) m	153.25	0.413	Memphis Sand	8.09
BS NP (2.75–3.00) m	153.00	0.351	Memphis Sand	6.34
GF L1 (0.00-0.25) m	154.75	0.130	Silty soil	1.43
GF NP (1.00–1.25) m	153.75	0.395	Sandy soil	7.57
GF NP (1.25–1.50) m	153.50	0.505	Sandy soil	10.94
GF NP (1.50–1.75) m	153.25	0.319	Sandy soil	5.49
GF NP (1.75–2.00) m	153.00	0.152	Memphis paleosol	1.81
GF NP (2.00–2.25) m	152.75	0.146	Memphis paleosol	1.70
GF NP (2.25–2.50) m	152.50	0.185	Memphis paleosol	2.43
GF NP (2.50–2.75) m	152.25	0.180	Memphis paleosol	2.33

GF NP (2.75–3.00) m	152.00	0.313	Memphis Sand	5.34
SS2 NP (0.00-0.25) m	159.55	0.140	Loess	1.60
SS2 NP (0.25-0.50) m	159.30	0.126	Loess	1.36
SS2 NP (0.50-0.75) m	159.05	0.123	Loess	1.32
SS2 NP (0.75–1.00) m	158.80	0.119	Loess	1.25
SS2 NP (1.00–1.25) m	158.55	0.145	Loess	1.68
SS2 NP (1.25–1.50) m	158.30	0.145	Loess	1.68
SS2 NP (1.50–1.75) m	158.05	0.137	Loess	1.55
SS2 NP (1.75–2.00) m	157.80	0.147	Loess	1.72
SS2 NP (2.00–2.25) m	157.55	0.170	Sandy paleosol	2.14
VF NP (0.00-0.25) m	144.75	0.100	Silty alluvium	0.96
VF NP (0.25-0.50) m	144.50	0.104	Silty alluvium	1.02
VF NP (0.50-0.75) m	144.25	0.102	Silty alluvium	0.99
VF NP (0.75–1.00) m	144.00	0.104	Silty alluvium	1.02
VF NP (1.00–1.25) m	143.75	0.092	Silty alluvium	0.85
VF NP (1.25–1.50) m	143.50	0.088	Silty alluvium	0.80
VF NP (1.50–1.75) m	143.25	0.089	Silty alluvium	0.81
VF NP (1.75–2.00) m	143.00	0.095	Silty alluvium	0.89
VF NP (2.00–2.25) m	142.75	0.095	Silty alluvium	0.89
VF NP (2.25–2.50) m	142.50	0.104	Silty alluvium	1.02
VF NP (2.50–2.75) m	142.25	0.123	Silty alluvium	1.32
VF NP (2.75–3.00) m	142.00	0.171	Silty alluvium	2.16
DPW BH 0.50 m	118.50	0.261	Sandy Alluvium	4.07
DPW BH 1.00 m	118.00	0.260	Sandy Alluvium	4.04
DPW BH 1.50 m	117.50	0.327	Sandy Alluvium	5.70
DPW BH 2.00 m	117.00	0.321	Sandy Alluvium	5.54
DPW BH 2.50 m	116.50	0.346	Sandy Alluvium	6.20
DPW BH 3.00 m	116.00	0.404	Memphis Sand	7.83
DPW BH 3.50 m	115.50	0.437	Memphis Sand	8.81
SS2 BH (11.6–12.2) m	147.61	0.135	Memphis Sand	1.51
SS2 BH (23.9–24.4) m	135.42	0.168	Memphis Sand	2.10
SS2 BH (34.5–35.1) m	124.75	0.216	Memphis Sand	3.06
SS2 BH (36.0–36.6) m	123.22	0.205	Memphis Sand	2.83
SS2 BH (57.6–57.9) m	101.89	0.132	Memphis Sand	1.46
VFW BH (9.1–9.8) m	125.55	0.160	Memphis Sand	1.95
VFW BH (14.6–15.2) m	120.06	0.231	Memphis Sand	3.38
VFW BH (23.8–25.3) m	110.00	0.125	Memphis Sand	1.35
VFW BH (25.3–25.9) m	109.39	0.133	Memphis Sand	1.48
VFW BH (29.3–29.9) m	105.43	0.165	Memphis Sand	2.04
DPW (Slug Test 1)	118.78	N/A	Memphis Sand	1.49
DPW (Slug Test 2)	118.78	N/A	Memphis Sand	1.46
SS2 (Slug Test 1)	113.84	N/A	Memphis Sand	4.88
SS2 (Slug Test 2A)	113.84	N/A	Memphis Sand	9.14
SS2 (Slug Test 2B)	113.84	N/A	Memphis Sand	7.62
SS2 (Slug Test 2C)	113.84	N/A	Memphis Sand	4.88
SS2 (Slug Test 2D)	113.84	N/A	Memphis Sand	0.73
SS2 (Slug Test 3)	113.84	N/A	Memphis Sand	2.26
SS2 (Slug Test 4)	113.84	N/A	Memphis Sand	0.73

Appendix C. Supplementary data

Supplementary material related to this article can be found, in the online version, at doi:https://doi.org/10.1016/j.ejrh.2020.100667.

References

Allen, R.G., Walter, I.A., Elliot, R.L., Howell, T.A., Itenfisu, D., Jensen, M.E., Snyder, R., 2005. The ASCE standardized reference evapotranspiration equation. ASCE Am. Soc. Civil Eng.

Allison, G.B., Hughes, M.W., 1978. The use of environmental chloride and tritium to estimate total recharge to an unconfined aquifer. Aust. J. Soil Res. 16, 181–195.

Allison, G.B., Hughes, M.W., 1983. The use of natural tracers as indicators of soil-water movement in a temperate semi-arid region. J. Hydrol. 60, 157–173.

Arthur, J.K., Taylor, R.E., 1998. Ground-water flow analysis of the Mississippi Embayment aquifer system, South-Central United States. U.S. Geological Survey Professional Paper 1416-I.

Bailey, Z.C., 1993. Hydrology of the Jackson, Tennessee, area and delineation of areas contributing ground water to the Jackson well fields. U.S. Geological Survey Water Resources Investigations Report 92-4146.

Bayer, R., Schlosser, P., Bönisch, G., Rupp, H., Zaucker, F., Zimmek, G., 1989. Performance and blank components of a mass spectrometric system for routine measurement of helium isotopes and tritium by the ^{3}He in-growth method. Sitzungsberichte der Heidelberger Akademie der Wissenschaften, Mathematisch-naturwissenschaftliche Klasse 5, 241–279.

Bouwer, H., Rice, R.C., 1976. A slug test method for determining hydraulic conductivity of unconfined aquifers with completely or partially penetrating wells. Water Resour. Res. 12 (3), 423–428.

Bradley, M.W., 1991. Ground-water hydrology and the effects of vertical leakage and leachate migration on ground-water quality near the Shelby County landfill, Memphis, Tennessee. U.S. Geological Survey Water-Resources Investigations Report 90-4075.

Brahana, J.V., Broshears, R.E., 2001. Hydrogeology and ground-water flow in the Memphis and Fort Pillow aquifers in the Memphis area, Tennessee. U.S. Geological Survey Water Resources Investigations Report 89-4131.
Brock, C.F., 2012. Geologic Mapping of the Macon and Moscow SE 7.5-minute Quadrangles With Sedimentological and Petrological Analysis of the Memphis sand. Masters Thesis. University of Memphis, Memphis, Tennessee.
Burnette, D.J., Stahle, D.W., 2013. Historical perspective on the dust bowl drought in the central United States. Climate Change 116 (3-4), 479–494. https://doi.org/10.1007/s10584-012-0525-2.
Bursi, J., 2015. Recharge Pathways and Mechanisms to the Memphis aquifer. Masters Thesis. University of Memphis, Memphis, Tennessee.
Busenberg, E., Plummer, L.N., 2000. Dating young ground water with sulfur hexafluoride: natural and anthropogenic sources of sulfur hexafluoride. Water Resour. Res. 36 (10), 3011–3030.
Carmichael, J.K., Kingsbury, J.A., Larsen, D., Schoefernacker, S., 2018. Preliminary evaluation of the hydrogeology and groundwater quality of the Mississippi River Valley alluvial aquifer and Memphis aquifer at the Tennessee Valley Authority Allen Power Plants, Memphis, Shelby County, Tennessee. U.S. Geological Survey Open-File Report 2018–1097. https://doi.org/10.3133/ofr20181097.
Clarke, W.B., Jenkins, W.J., Top, Z., 1976. Determination of tritium by mass spectrometric measurements of ^{3}He. Int. J. Appl. Radioactive Isotopes 27, 515–522.
Cook, P.G., Böhlke, J.K., 2000. Determining timescales for groundwater flow and solute transport. In: Cook, P.G., Herczeg, A.L. (Eds.), Environmental Tracers in Subsurface Hydrology. Kluwer, Boston, pp. 1–30.
Dafny, E., Šimúnek, J., 2016. Infiltration in layered loessial deposits: revised numerical simulations and recharge assessment. J. Hydrol. 538, 339–354. https://doi.org/10.1016/j.jhydrol.2016.04.029.
Dawes, W., Ali, R., Varma, S., Emelyanova, I., Hodgson, G., McFarlane, D., 2012. Modelling the effects of climate and land cover change on groundwater recharge in south-west Western Australia. Hydrol. Earth Syst. Sci. 16, 2709–2722. https://doi.org/10.5194/hess-16-2709-2012.
De Vries, J.J., Simmers, I., 2002. Groundwater recharge: an overview of processes and challenges. Hydrogeol. J. 10 (1), 5–17.
Deng, L., Wang, W., Yanjun, C., Hu, A., Tan, L., 2015. Groundwater diffuse recharge and its response to climate changes in semi-arid northwestern China. Terr. Atmos. Ocean. Sci. 26 (4), 451–461. https://doi.org/10.3319/TAO.2015.03.18.01(Hy).
Dingman, S.L., 2002. Physical Hydrology. Prentice-Hall, New Jersey.
Fetter, C.W., 2001. Applied Hydrogeology, 4th ed. Prentice Hall, New Jersey.
Flowers, R.L., 1964. Soil Survey of Fayette County, Tennessee. U.S. Department of Agriculture.
Gates, J.B., Scanlon, B.R., Mu, X., Zhang, L., 2011. Impacts of soil conservations on groundwater recharge in the semi-arid Loess Plateau, China. Hydrogeol. J. 19, 865–875. https://doi.org/10.1007/s10040-011-0716-3.
Gates, J.B., Steele, G.V., Nasta, P., Szilagyi, J., 2014. Lithologic influences on groundwater recharge through incised glacial till from profile to regional scales: evidence from glaciated Eastern Nebraska. Water Resour. Res. 50, 1–16. https://doi.org/10.1002/2013WR014073. 2014.
Gee, G.W., Bauder, J.W., 1986. Particle-size analysis. In: Klute, A. (Ed.), Methods of Soil Analysis, Part 1: Physical and Mineralogical Methods. American Society of Agronomy, pp. 383–411.
Gentry, R.W., McKay, L., Thonnard, N., Anderson, J.L., Larsen, D., Carmichael, J.K., Solomon, K., 2006. Novel techniques for investigating recharge to the Memphis aquifer. Am. Water Works Assoc., 91137F.
Gerginov, P., Orehova, T., Petrova, V., Antonov, D., 2018. Moisture regime in the upper part of the loess complex in North-eastern Bulgaria. Rev. Bulg. Geol. Soc. 79 (3), 139–140.
Grimley, D.A., Larsen, D., Kaplan, S.W., Yansa, C.H., Curry, B.B., Oches, E.A., 2009. A multi-proxy palaeoecological and palaeoclimatic record within full glacial lacustrine deposits, western Tennessee, USA. J. Quat. Sci. 24 (8), 960–981.
Huang, T., Pang, Z., Liu, J., Ma, J., Gates, J., 2017. Groundwater recharge mechanism in an integrated tableland of the Loess Plateau, northern China: insights from environmental tracers. Hydrogeol. J. 25, 2049–2065. https://doi.org/10.1007/s10040-017-1599-8.
Johnston, C.D., 1987a. Preferred water flow and localized recharge in a variable regolith. J. Hydrol. 94, 129–142.
Johnston, C.D., 1987b. Distribution of environmental chloride in relation to subsurface hydrology. J. Hydrol. 94, 67–88.
Jurgens, B.C., Böhlke, J.K., Eberts, S.M., 2012. TracerLPM (version 1): an excel® workbook for interpreting ground water age distributions from environmental tracer data. U.S. Geological Survey Techniques and Methods Report 4-F3.
Kalhoro, S.A., Ding, K., Zhang, B., Chen, W., Hua, R., Shar, A.H., Xu, X., 2018. Soil infiltration rate of forestland and grassland over different vegetation restoration periods at Loess Plateau in northern hilly areas of China. Landsc. Ecol. Eng. 15, 91–99. https://doi.org/10.1007/s11355-018-0363-0.
Kang, C.-M., Gupta, T., Ruiz, P.A., Wolfson, J.M., Ferguson, S.T., Lawrence, J.E., Rohr, A.C., Godleski, J., Koutrakis, P., 2011. Aged particles derived from emissions of coal-fired power plants: the TERESA field results. Inhal. Toxicol. 23 (sup2), 11–30. https://doi.org/10.3109/08958371003728040.
Kilpatrick, F.A., Schneider, V.R., 1983. Use of flumes in measuring discharge: United State Geological Survey. Techn. Water Resour. Investig. 03–A14.
Kingsbury, J.A., 2018. Altitude of the potentiometric surface, 2000-2015, and historical water- level changes in the Memphis Area, Tennessee. U.S. Geol. Surv. Sci. Investig. Map 3415https://doi.org/10.3133/sim3415. 1 sheet.
Lajtha, K., Jones, J., 2013. Trends in cation, nitrogen, sulfate, and hydrogen ion concentrations in precipitation in the United States and Europe from 1978 to 2010: a new look at an old problem. Biogeochemistry 116, 303–334. https://doi.org/10.1007/s10533-013-9860-2.
Larsen, D., Brock, C.F., 2014. Sedimentology and petrology of the eocene Memphis sand and younger terrace deposits in surface exposures of Western Tennessee. Southeastern Geol. 50 (4), 193–214.
Larsen, D., Waldron, B., 2020. Low-level soluble chloride extraction in soil. submission. MethodsX: MEX-D-20-00037.
Larsen, D., Gentry, R.W., Solomon, D.K., 2003. The geochemistry and mixing of leakage in a semi-confined aquifer at a municipal well field, Memphis, Tennessee, USA. Appl. Geochem. 18 (7), 1043–1063.
Larsen, D., Morat, J., Waldron, B., Ivey, S., Anderson, J.L., 2013. Stream loss contributions to a municipal water supply aquifer, Memphis, Tennessee. Environ. Eng. Geosci. 19, 265–287.
Law, C.S., Watson, A.J., Liddicoat, M.I., 1994. Automated vacuum analysis of sulfur hexafluoride in seawater: derivation of the atmospheric trend (1979-1993) and potential as a transient tracer. Mar. Chem. 48, 57–69.
Li, W., Wang, L., Qiao, Y., Lin, J.-Y., Wang, M., Chang, L., 2015. Effects of atmosphere on the release behavior of alkali and alkaline earth metals during coal oxy-fuel combustion. Fuel 139, 164–170. https://doi.org/10.1016/j.fuel.2014.08.056.
Lin, R., Wei, K., 2006. Tritium profiles of pore water in the Chinese loess unsaturated zone: implications for estimation of groundwater recharge. J. Hydrol. 328, 192–199. https://doi.org/10.1016/j.jhydrol.2005.12.010.
Lumsden, D.N., Hundt, K.R., Larsen, D., 2009. Petrology of the Memphis sand in the northern Mississippi Embayment. Southeastern Geol. 46 (3), 121–133.
Macfarlane, P.A., Clark, J.F., Davisson, M.L., Hudson, G.B., Whittemore, D.O., 2000. Late-Quaternary recharge determined from chloride in shallow groundwater in the central Great Plains. Quat. Res. 53, 167–174.
Maupin, M.A., Kenny, J.F., Hutson, S.S., Lovelace, J.K., Barber, N.L., Linsey, K.S., 2014. Estimated use of water in the United States in 2010: U.S. Geol. Surv. Circular 1405, 56 p.. https://doi.org/10.3133/cir1405.
McKee, P.W., Clark, B.R., 2003. Development and calibration of a ground-water flow model for the Sparta aquifer of southeastern Arkansas and north-central Louisiana and simulated response to withdrawals, 1998-2027. U.S. Geological Survey Water Resources Investigations Report 03-4132.
Michel, R.M., 2004. Tritium hydrology of the Mississippi River Basin. Hydrol. Process. 18 (7), 1255–1269.
Moore, G.K., Brown, D.L., 1969. Stratigraphy of the Fort pillow test well, Lauderdale County, Tennessee. Tennessee Division of Geology Report of Investigations. pp. 26.
National Weather Service, 2019. Memphis International Airport, Memphis, Tennessee. (Accessed May 2019). https://forecast.weather.gov/MapClick.php?lat=35.1&lon=-90#.XRPzSOhKhPa.
NOAA, 2015. National centers for environmental information, Ames plantation, TN US. Station Data Viewer. (Accessed 2014-2015). http://www.ncdc.noaa.gov/cdo-web/datasets/GHCND/stations/GHCND:USC00400137/detail.

Nolan, B.T., Healy, R.W., Taber, P.E., Perkins, K., Hitt, K.J., Wolock, D.M., 2007. Factors influencing ground-water recharge in the eastern United States. J. Hydrol. 332 (1-2), 187–205.
Parks, W.S., 1990. Hydrogeology and preliminary assessment of the potential for contamination of the Memphis aquifer in the Memphis area, Tennessee. United States Geological Survey Water Resources Investigations Report 90-4092.
Parks, W.S., Carmichael, J.K., 1990. Geology and ground-water resources of the Memphis Sand in western Tennessee. United States Geological Survey Water-Resources Investigations Report 88-4182.
Pigati, J.S., McGeehin, J.P., Muhs, D.R., Grimley, D.A., Nekola, J.C., 2014. Radiocarbon dating loess deposits in the Mississippi Valley using terrestrial gastropod shells (Polygyridae, Helicinidae, and Discidae). Aeolian Res. 16, 25–33.
Prill, R.C., 1977. Movement of moisture in the unsaturated zone in a loess-mantled area, southwestern Kansas. United States Geological Survey Professional Paper 1020.
Rodbell, D.T., Forman, S.L., Pierson, J., Lynn, W.C., 1997. Stratigraphy and chronology of Mississippi Valley loess in western Tennessee. Geol. Soc. Am. Bull. 109, 1134–1148.
Rushton, K.R., 1988. Numerical and conceptual models for recharge estimation in arid and semi-arid zones. In: Simmers, I. (Ed.), Estimation of Natural Groundwater Recharge. NATO ASI Series C 222. Reidel, Dordrecht, pp. 223–238.
Rushton, K.R., Ward, C., 1979. The estimation of groundwater recharge. J. Hydrol. 41, 345–361.
Russell, E.E., Parks, W.S., 1975. Stratigraphy and outcropping Upper Cretaceous, Paleocene, and Lower Eocene in Western Tennessee (including descriptions of younger fluvial deposits). Division of Geology, Bulletin. State of Tennessee Department of Conservation, pp. 75.
Russo, S.L., Zavattaro, L., Acutis, M., Zuppi, G.M., 2003. Chloride profile technique to estimate water movement through unsaturated zone in a cropped area in sub-humid climate (Po Valley – NW Italy). J. Hydrol. 270, 65–74.
Sanford, W.E., Selnick, D.L., 2012. Estimation of evapotranspiration across the conterminous United States using a regression with climate and land-cover data. J. Am. Water Resour. Assoc. 49, 217–230. https://doi.org/10.1111/jawr.12010.
Santoni, S., Huneau, F., Garel, E., Vergnaud-Ayraud, V., Labasque, T., Aquilina, L., Jaunat, J., Celle-Jeanton, H., 2016. Residence time, mineralization process and groundwater origin within a carbonate coastal aquifer with a thick unsaturated zone. J. Hydrol. 540, 50–63.
Scanlon, B.R., Healy, R.H., Cook, P.G., 2002. Choosing appropriate techniques for quantifying groundwater recharge. Hydrogeol. J. 10 (1), 18–39.
Schlosser, P., Stute, M., Dorr, H., Sonntag, C., Munnich, K.O., 1988. Tritium/^{3}He dating of shallow groundwater. Earth Planet. Sci. Lett. 89, 353–362.
Seiler, R.I., 1999. A Chemical Signature for Ground Water Contaminated by Domestic Wastewater. Ph.D. dissertation. University of Nevada, Reno, Nevada.
Sharma, M.L., Hughes, M.W., 1985. Groundwater recharge estimation using chloride, deuterium, and oxygen-18 profiles in the deep coastal sands of Western Australia. J. Hydrol. 81, 93–109.
Shepherd, R.G., 1989. Correlations of permeability and grain size. Groundwater 27 (5), 618–730.
Simco, W.A., 2018. Recharge of the Memphis aquifer in an Incised Urban Watershed. Masters Thesis. University of Memphis, Memphis, Tennessee.
Smith, S.R., 2019. Recharge of the Memphis aquifer in an Incised Urban Watershed: Implications of Impervious Surfaces and Stream Incision. Masters Thesis. University of Memphis, Memphis, Tennessee.
Smith, W.S., Gruber, C.W., 1966. Atmospheric emissions from coal combustion: an inventory guide. Public Health Service Publication. pp. 999-AP-24.
Solomon, D.K., Cook, P.G., 1995. Transport of atmospheric trace gases to the water table: implications for groundwater with chlorofluorocarbons and dating krypton 85. Water Resour. Res. 31, 263–270. https://doi.org/10.1029/94WR02232.
Solomon, D.K., Cook, P.G., 2000. ^{3}H and ^{3}He. In: Cook, P.G., Herczeg, A.L. (Eds.), Environmental Tracers in Subsurface Hydrology. Kluwer Academic, Boston, pp. 397–424.
Sophocleous, M.A., 1991. Combining the soilwater balance and water-level fluctuation methods to estimate natural ground-water recharge: practical aspects. J. Hydrol. 124, 229–241.
Sophocleus, M., Perry, C.A., 1985. Experimental studies in natural groundwater-recharge dynamics—the analysis of observed recharge events. J. Hydrol. 81, 287–332.
Steenhuis, T.S., Jackson, C.D., Kung, S.K., Brutsaert, W., 1985. Measurement of groundwater recharge in eastern Long Island, New York, USA. J. Hydrol. 79, 145–169.
Stricker, V.A., 1983. Base flow of streams in the outcrop area of southeastern sand aquifer: South Carolina, Georgia, Alabama, and Mississippi. United States Geological Survey Water Resources Investigations Report. pp. 83–4106.
United States Geological Survey, 2015. National Water Information System (USGS Water Data for the Nation). (Accessed August 2015). http://waterdata.usgs.gov/tn/nwis/inventory/?site_no=07030392&agency_cd=USGS/.
Van Arsdale, R.B., Bresnahan, R.P., McCallister, N.S., Waldron, B., 2008. The Upland Complex of the Central Mississippi River Valley: its origin, denudation, and possible role in reactivation of the New Madrid seismic zone. In: In: Stein, S., Mazzotti, S. (Eds.), Continental Intraplate Earthquakes: Science, Hazard, and Policy Issues. Geological Society of America Special Paper 425. pp. 177–192.
Wanninkhof, R., Ledwell, R., 1991. Analysis of sulfur hexafluoride in seawater. J. Geophys. Res. 96 (C), 8733–8740.
Weinthal, E., Vengosh, A., Marei, A., Gutierrez, A., Kloppmann, W., 2005. The water crisis in the Gaza strip: prospects for resolution. Ground Water 43 (5), 653–660.
Wilson, R.D., Mackay, D.M., 1993. The use of sulphur hexafluoride as a conservative tracer in saturated sandy media. Ground Water 31 (5), 719–724.
Wood, W.W., 1999. Use and misuse of the chloride-mass balance method in estimating ground water recharge. Ground Water 1, 2–3.
Wood, W.W., Sanford, W.E., 1995. Chemical and isotopic method for quantifying ground-water recharge in a regional, semiarid environment. Ground Water 33 (3), 458–486.
Wu, J., Zhang, R., Yang, J., 1996. Analysis of rainfall-recharge relationships. J. Hydrol. 177 (1-2), 143–160.
WU, 2015. Weather underground. The Weather Company, LLC, Frazier Road KTNROSSV2, Weather History. (Accessed 2015). https://www.wunderground.com/personal-weather-station/dashboard?ID=KTNROSSV2#history/s20141019/e20141019/mdaily.
Zhang, Z., Li, M., Si, B., Feng, H., 2018. Deep-rooted apple trees decrease groundwater recharge in the highland region of the Loess Plateau, China. Sci. Total Environ. 622-623, 584–593. https://doi.org/10.1016/j.scitotenv.2017.11.230.
Zotarelli, L., Dukes, M.D., Romero, C.C., Migliaccio, K.W., Morgan, K.T., 2009. Step by Step Calculation of the Penman-Monteith Evapotranspiration (Fao-56 Method). University of Florida, pp. AE459 IFAS Extension.